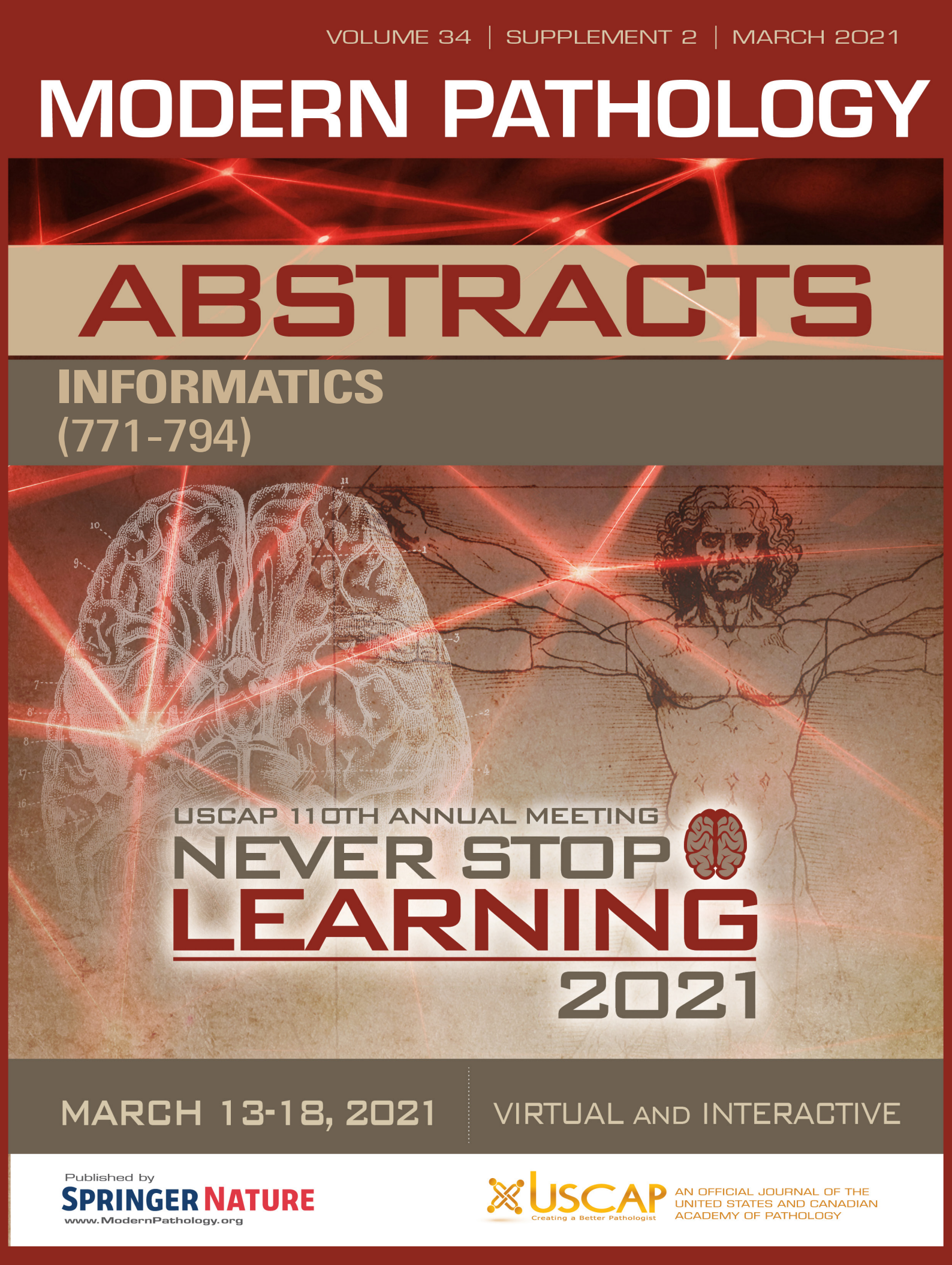


# MODERN PATHOLOGY

## ABSTRACTS

INFORMATICS  
(771-794)



USCAP 110TH ANNUAL MEETING  
**NEVER STOP**  
**LEARNING**  
**2021**

MARCH 13-18, 2021

VIRTUAL AND INTERACTIVE

Published by  
**SPRINGER NATURE**  
[www.ModernPathology.org](http://www.ModernPathology.org)

 **USCAP** AN OFFICIAL JOURNAL OF THE  
UNITED STATES AND CANADIAN  
ACADEMY OF PATHOLOGY  
Creating a Better Pathologist

**EDUCATION COMMITTEE**

**Jason L. Hornick**  
Chair

**Rhonda K. Yantiss, Chair**  
Abstract Review Board and Assignment Committee

**Kristin C. Jensen**  
Chair, CME Subcommittee

**Laura C. Collins**  
Interactive Microscopy Subcommittee

**Raja R. Seethala**  
Short Course Coordinator

**Ilan Weinreb**  
Subcommittee for Unique Live Course Offerings

**David B. Kaminsky**  
(Ex-Officio)  
**Zubair W. Baloch**  
**Daniel J. Brat**  
**Sarah M. Dry**  
**William C. Faquin**  
**Yuri Fedoriw**  
**Karen Fritchie**  
**Jennifer B. Gordetsky**  
**Melinda Lerwill**  
**Anna Marie Mulligan**

**Liron Pantanowitz**  
**David Papke,**  
Pathologist-in-Training  
**Carlos Parra-Herran**  
**Rajiv M. Patel**  
**Deepa T. Patil**  
**Charles Matthew Quick**  
**Lynette M. Sholl**  
**Olga K. Weinberg**  
**Maria Westerhoff**  
**Nicholas A. Zoumberos,**  
Pathologist-in-Training

**ABSTRACT REVIEW BOARD**

**Benjamin Adam**  
**Rouba Ali-Fehmi**  
**Daniela Allende**  
**Ghassan Allo**  
**Isabel Alvarado-Cabrero**  
**Catalina Amador**  
**Tatjana Antic**  
**Roberto Barrios**  
**Rohit Bhargava**  
**Luiz Blanco**  
**Jennifer Boland**  
**Alain Borczuk**  
**Elena Brachtel**  
**Marilyn Bui**  
**Eric Burks**  
**Shelley Caltharp**  
**Wenqing (Wendy) Cao**  
**Barbara Centeno**  
**Joanna Chan**  
**Jennifer Chapman**  
**Yunn-Yi Chen**  
**Hui Chen**  
**Wei Chen**  
**Sarah Chiang**  
**Nicole Cipriani**  
**Beth Clark**  
**Alejandro Contreras**  
**Claudio Cotta**  
**Jennifer Cotter**  
**Sonika Dahiya**  
**Farbod Darvishian**  
**Jessica Davis**  
**Heather Dawson**  
**Elizabeth Demicco**  
**Katie Dennis**  
**Anand Dighe**  
**Suzanne Dintzis**  
**Michelle Downes**

**Charles Eberhart**  
**Andrew Evans**  
**Julie Fanburg-Smith**  
**Michael Feely**  
**Dennis Firchau**  
**Gregory Fishbein**  
**Andrew Folpe**  
**Larissa Furtado**  
**Billie Fyfe-Kirschner**  
**Giovanna Giannico**  
**Christopher Giffith**  
**Anthony Gill**  
**Paula Ginter**  
**Tamar Giorgadze**  
**Purva Gopal**  
**Abha Goyal**  
**Rondell Graham**  
**Alejandro Gru**  
**Nilesh Gupta**  
**Mamta Gupta**  
**Gillian Hale**  
**Suntrea Hammer**  
**Malini Harigopal**  
**Douglas Hartman**  
**Kammi Henriksen**  
**John Higgins**  
**Mai Hoang**  
**Aaron Huber**  
**Doina Ivan**  
**Wei Jiang**  
**Vickie Jo**  
**Dan Jones**  
**Kirk Jones**  
**Neerja Kambham**  
**Dipti Karamchandani**  
**Nora Katabi**  
**Darcy Kerr**  
**Francesca Khani**

**Joseph Khoury**  
**Rebecca King**  
**Veronica Klepeis**  
**Christian Kunder**  
**Steven Lagana**  
**Keith Lai**  
**Michael Lee**  
**Cheng-Han Lee**  
**Madelyn Lew**  
**Faqian Li**  
**Ying Li**  
**Haiyan Liu**  
**Xiuli Liu**  
**Lesley Lomo**  
**Tamara Lotan**  
**Sebastian Lucas**  
**Anthony Magliocco**  
**Kruti Maniar**  
**Brock Martin**  
**Emily Mason**  
**David McClintock**  
**Anne Mills**  
**Richard Mitchell**  
**Neda Moatamed**  
**Sara Monaco**  
**Atis Muehlenbachs**  
**Bitu Naini**  
**Dianna Ng**  
**Tony Ng**  
**Michiya Nishino**  
**Scott Owens**  
**Jacqueline Parai**  
**Avani Pendse**  
**Peter Pytel**  
**Stephen Raab**  
**Stanley Radio**  
**Emad Rakha**  
**Robyn Reed**

**Michelle Reid**  
**Natasha Rekhman**  
**Jordan Reynolds**  
**Andres Roma**  
**Lisa Rooper**  
**Avi Rosenberg**  
**Esther (Diana) Rossi**  
**Souzan Sanati**  
**Gabriel Sica**  
**Alexa Siddon**  
**Deepika Sirohi**  
**Kalliopi Siziopikou**  
**Maxwell Smith**  
**Adrian Suarez**  
**Sara Szabo**  
**Julie Teruya-Feldstein**  
**Khin Thway**  
**Rashmi Tondon**  
**Jose Torrealba**  
**Gary Tozbikian**  
**Andrew Turk**  
**Evi Vakiani**  
**Christopher VandenBussche**  
**Paul VanderLaan**  
**Hannah Wen**  
**Sara Wobker**  
**Kristy Wolniak**  
**Shaofeng Yan**  
**Huihui Ye**  
**Yunshin Yeh**  
**Anjana Yeldandi**  
**Gloria Young**  
**Lei Zhao**  
**Minghao Zhong**  
**Yaolin Zhou**  
**Hongfa Zhu**

To cite abstracts in this publication, please use the following format: **Author A, Author B, Author C, et al. Abstract title (abs#). In "File Title." *Modern Pathology* 2021; 34 (suppl 2): page#**

**771 Remote Digital Pathology for Clinical Trials and Research During the COVID-19 Pandemic**

Umesh Bhanot<sup>1</sup>, Faruk Erdem Kombak<sup>1</sup>, Jordana Ray-Kirton<sup>1</sup>, Faye Taylor-Mason<sup>1</sup>, Asako Tanaka<sup>1</sup>, Song (Lillian) Xiaoqing<sup>1</sup>, Joachim Silber<sup>1</sup>, Michael Roehrl<sup>1</sup>  
<sup>1</sup>Memorial Sloan Kettering Cancer Center, New York, NY

**Disclosures:** Umesh Bhanot: None; Faruk Erdem Kombak: None; Jordana Ray-Kirton: None; Faye Taylor-Mason: None; Asako Tanaka: None; Song (Lillian) Xiaoqing: None; Joachim Silber: None; Michael Roehrl: None

**Background:** Healthcare organizations are faced with the challenge of maintaining essential services during the COVID-19 pandemic, while ensuring the safety of healthcare workers including pathologists and the laboratory personnel. The Precision Pathology Center (PPBC) at MSKCC is a central hub for specimen-driven clinical trials, biomarker development, molecular characterization, and research. Evaluation of tissues by a pathologist to assess tumor cellularity, inflammation, fibrosis, and necrosis, is essential for specimen-centered clinical trials. We describe our experience adopting digital pathology solutions and remote pathology review to avoid any interruptions in our services during the current healthcare emergency.

**Design:** Tissues for clinical trial and research are routinely evaluated by a pathologist. Normally, the evaluations are performed by the research pathologists on site. During the COVID-19 pandemic, this posed a challenge due to shutdowns and institutional safeguards to control the spread of the virus. Safety of pathologists and laboratory personnel was a major concern. Equally important was the concern for maintaining efficient patient care, so that patients on oncologic clinical trials could continue to receive specific experimental therapies. Our biobank routinely digitizes all tissue slides since 2017. The biobank slide digital archive comprises >42,000 slides with ~300 new cases added weekly. During the pandemic digital pathology systems and remote access for pathology review were operationalized. Whole slide images (WSI) were integrated into and launched within the biobank LIS. For remote review of WSI, consumer grade computers and monitors were connected to an institutional workstation via secure virtual private network (VPN).

**Results:** Digital pathology systems and remote access to WSI allowed pathology review for clinical trials and research to continue uninterrupted even during worst of the COVID-19 pandemic. Remote clinical trial slide review could be utilized for over 550 patients and 1,050 slides (90% of tissue requests for clinical trials) during the first 6 months starting March 2020. The pathologists were required to review glass slides on location only in those few cases where digital slides were not available. Integration of digital pathology systems and the LIS with research tissue biobanking systems allowed remote pathology review of banked tissue histology ensuring the quality of banked tissues specimen as well.

**Conclusions:** Digital pathology solutions and remote pathology review allowed uninterrupted PPBC research and clinical trial operations during the COVID-19 pandemic while ensuring the safety of pathologists and laboratory personnel. Rapid IT development and custom-programmed integration of our research LIS with digital imaging workflows proved crucial during this healthcare emergency.

**772 Can Deep Learning Artificial Intelligence Assist Busy Pathologists in Screening for Colorectal Malignancies?**

Xiufen Chen<sup>1</sup>, Zitong Zhao<sup>1</sup>, Jan Sauer<sup>2</sup>, Sahil Ajit Saraf<sup>2</sup>, Rajasa Jialdasani<sup>2</sup>, Kaveh Taghipour<sup>2</sup>, Aneesh Sathe<sup>2</sup>, Li Yan Khor<sup>1</sup>, Kiat Hon Lim<sup>1</sup>, Wei-Qiang Leow<sup>1</sup>  
<sup>1</sup>Singapore General Hospital, Singapore, Singapore, <sup>2</sup>Qritive Pte. Ltd., Singapore, Singapore

**Disclosures:** Wei-Qiang Leow: None

**Background:** Colorectal cancer is one of the top three cancers afflicting men and women worldwide, with an estimated 1.8 million people diagnosed in 2018. As colonoscopies become more accessible and affordable, colorectal biopsies account for a great part of the histopathology laboratory workload. Artificial Intelligence (AI) promises to streamline workflow, and improve cancer detection and classification; enabling busy pathologists to focus on higher order decision-making tasks. We trained and validated a unique AI deep learning model as an assistive tool to screen for colonic malignancies in colorectal specimens.

**Design:** The study cohort consists of Whole Slide Images (WSI) obtained from 294 colorectal specimens. Utilising Qritive's unique deep learning model based on a region-based convolutional network (Mask-RCNN) architecture with a ResNet-50 feature extraction backbone that provides glandular segmentation and a classical machine learning classifier, we first trained our glandular segmentation deep learning model using pathologist's annotations on a training cohort of 66191 image tiles extracted from 39 WSIs (8 biopsies and 31 resections). We then applied a classical machine learning-based slide classifier that sorted the WSIs into low-risk (benign, inflammation) and high-risk (dysplasia, malignancy) categories. We then further trained the composite AI-model's performance on a larger cohort of 105 resections WSIs and validated our findings on a cohort of 150 biopsies WSIs, against the classifications of two independently blinded pathologists. We evaluated the area under the receiver-operator characteristic curve (AUC) and other performance metrics.

**Results:** The AI-model achieved an AUC of 0.917 in biopsies WSIs. Notably the AI-model achieved excellent sensitivity (97.4%) in detection of high-risk features of dysplasia and malignancy, but demonstrated lesser specificity (60.3%). Our ongoing review suggests that our composite AI-model is imperfect in situations of abundant mucin and low grade dysplastic glands, resulting in the higher than expected false positive rates.

Figure 1 - 772

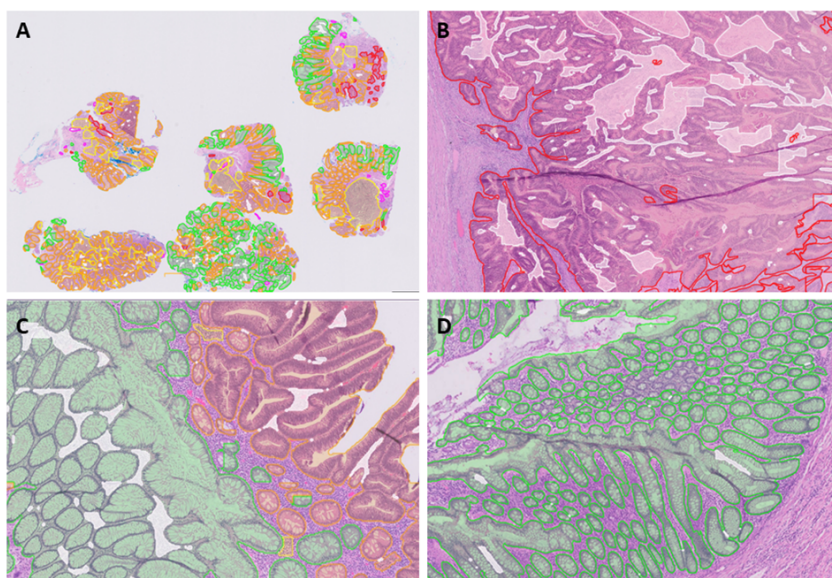


Figure 1. The unique glandular segmentation output of our AI-model. The AI-annotated colors are: red-malignant glands; orange-dysplastic glands; green-benign glands; yellow-inflammation; purple-blood vessels.

**Conclusions:** We demonstrate that our unique composite AI-model incorporating both a glandular segmentation deep learning model and a classical machine learning classifier has promising ability in picking up high risk colorectal features (Figure 1). The concomitant high sensitivity highlights its role as a potential screening tool in assisting busy pathologists by outlining the dysplastic and malignant glands. Ongoing calibration and training of our composite AI-model will improve its accuracy in risk classification of colorectal specimens.

### 773 Development and Validation of Deep Learning-Based Pathologic Classification of Immune Phenotype in Non-Small Cell Lung Cancer

Sangjoon Choi<sup>1</sup>, Yeon Bi Han<sup>2</sup>, Wonjun Yoon<sup>3</sup>, Hoon Kim<sup>3</sup>, Donggeun Yoo<sup>3</sup>, Kyunghyun Paeng<sup>3</sup>, Chan-Young Ock<sup>3</sup>, Hyojin Kim<sup>2</sup>, Seokhwi Kim<sup>4</sup>

<sup>1</sup>Samsung Medical Center, Seoul, South Korea, <sup>2</sup>Seoul National University Bundang Hospital, Seongnam, South Korea, <sup>3</sup>Lunit Inc., Seoul, South Korea, <sup>4</sup>Ajou University School of Medicine, Suwon, South Korea

**Disclosures:** Sangjoon Choi: None; Yeon Bi Han: None; Wonjun Yoon: *Employee*, Lunit, Inc.; Hoon Kim: *Employee*, Lunit, Inc.; *Stock Ownership*, Lunit, Inc.; Donggeun Yoo: None; Kyunghyun Paeng: *Stock*

Ownership, Lunit Inc.; Employee, Lunit Inc.; Chan-Young Ock: Employee, Lunit, Inc.; Stock Ownership, Lunit, Inc.; Hyojin Kim: None; Seokhwi Kim: None

**Background:** Distribution of tumor-infiltrating lymphocytes (TIL) intratumorally or excluded to peritumoral stroma is a key factor for predicting response of immunotherapy. However, there is no pathologic consensus for the classification of TIL distribution, or immune phenotype so far. Therefore, development of consensus guideline and utilizing a deep learning model to classify immune phenotype is highly interested.

**Design:** Three-immune phenotype (3-IP) consensus guideline were adopted from the Proposal from the International Immunooncology Biomarkers Working Group and related literatures. A total of 170 H&E stained whole slide images of non-small cell lung cancer (NSCLC) from Cureline (CA) were dissected into small patch images sized 0.05 mm<sup>2</sup>. Two pathologists annotated 3-IP of patch images included in both training and validation sets, and concordantly annotated patches were considered as ground-truth. As 3-IP classifier, a deep learning model called ResNet-18 comprising 18 convolutional layers is used, and the cross-entropy was defined as the loss function. To estimate interobserver variation, another two independent pathologists annotated 3-IP following the guideline. Deep learning model also predict 3-IP of validation set.

**Results:** 3-IP was defined as follows: *inflamed* phenotype as > 25 intratumoral TIL per high power field (HPF) or > 95 stromal TIL per HPF in intratumoral stroma; *excluded* phenotype as > 95 stromal TIL per HPF in peritumoral stroma; *desert* phenotype as tumors that do not fulfill the TIL cutoffs of *inflamed* or *excluded* (Figure 1). Patches with less than 20 cancer cells or showing crush artifacts are allocated in unknown category. The proportion of 3-IP annotated by pathologists was comparable in training (N=1,823) and validation (N=382) patch images: 30.3% and 25.7% as *inflamed*; 26.3% and 30.1% as *excluded*; 19.0% and 17.8% as *desert*, respectively. The accurate prediction of 3-IP by the deep learning model was increased to achieve 92.4% in validation set as we used more images for training set up to N=1,823 (Figure 2). In the same validation set, two independent pathologists annotated 3-IP with concordance rates of 85.3% and 75.7%, respectively.

Figure 1 - 773

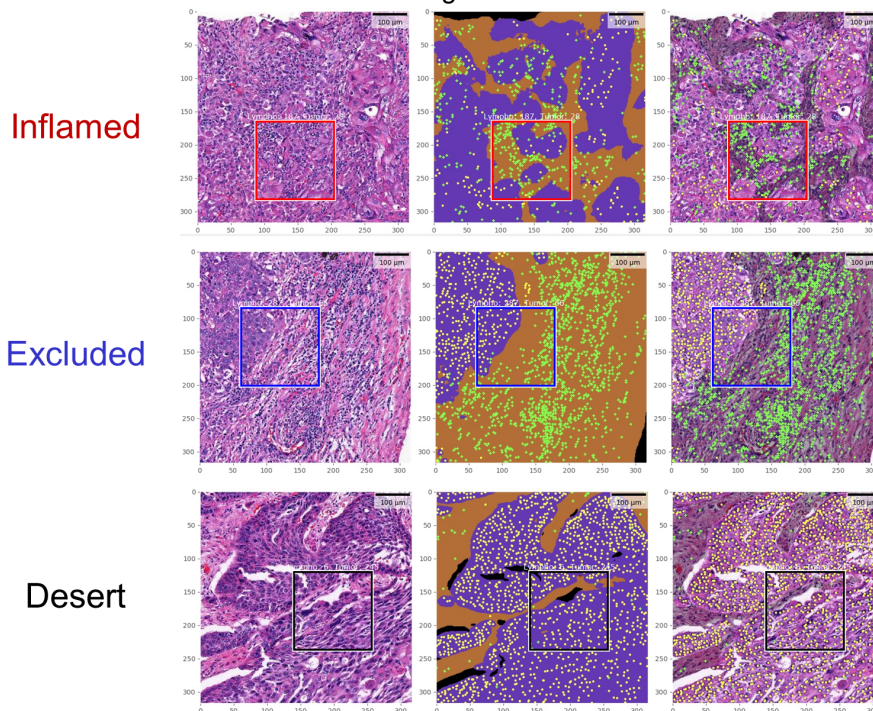
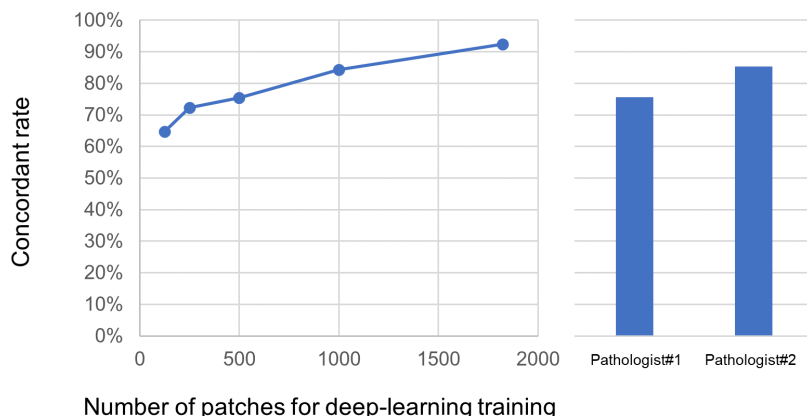


Figure 2 - 773



**Conclusions:** Pathologic guideline of 3-IP can reflect the distribution of TIL, which can be objectively reproduced by independent pathologists. A deep-learning model can also accurately predict 3-IP, which enables it to be utilized as a novel biomarker of immunotherapy in the digital pathology era.

**774 Diagnostic Concordance Between Whole Slide Imaging and Light Microscopy of Bone Marrow Core Biopsies**

Mehrvash Haghighi<sup>1</sup>, Max Signaevsky<sup>2</sup>, Siraj El Jamal<sup>2</sup>, Christian Salib<sup>2</sup>, XiangFu Zhang<sup>2</sup>, Mega Lahori<sup>3</sup>, Ricky Kwan<sup>1</sup>, Shafinaz Hussein<sup>1</sup>

<sup>1</sup>Mount Sinai Hospital, New York, NY, <sup>2</sup>Icahn School of Medicine at Mount Sinai, New York, NY, <sup>3</sup>Mount Sinai Morningside West Hospital, New York, NY

**Disclosures:** Mehrvash Haghighi: None; Max Signaevsky: None; Siraj El Jamal: None; Christian Salib: None; XiangFu Zhang: None; Mega Lahori: None; Ricky Kwan: None; Shafinaz Hussein: None

**Background:** Digital pathology is a rapidly growing technology in surgical pathology. However, the use in hematopathology has been limited due to concerns about quality of WSI for morphologic interpretation. The aim of this study was to determine the diagnostic concordance of Whole slide imaging (WSI) and light microscopy (LM) in bone marrow biopsy specimens. We implemented digital pathology for primary diagnosis in our lab since January 2020 and all bone marrow core biopsies and associated immunostains and special stains are scanned.

**Design:** We selected 180 bone marrow core biopsy cases examined from June to September of 2020. To evaluate the concordance for the diagnosis rendered by WSI and LM, we measured the inter-observer concordance with Cohen’s kappa coefficient (k). We also compared the evaluation of different factors such as bone marrow cellularity, myeloid, erythroid, M: E ratio, number and morphology of megakaryocytes, percentage of blasts and lymphoid cells, plasma cell cellularity, and morphology, and reticulin and trichrome grading. The quality of 1610 individual digital images was examined, and associated artifacts and technical issues documented.

**Results:** The bone marrow biopsy results showed following diagnosis: plasma cell neoplasm (n=108, 60%), unremarkable (n=31, 17%), myelodysplastic syndrome (n=10, 6%), lymphoma (n=9, 8%), myeloproliferative disease (n=7, 4%), metastatic carcinoma (n=1) and insufficient for diagnosis (n=14, 8%). There was a 100% concordance intraobserver rate in the final diagnosis ( $p<0.001$ ). The degree of intraobserver agreement in the interpretation of megakaryocytic morphology was higher ( $k=0.735$ ) compared to plasma cells ( $k=0.452$ ). A thorough examination of slides showed a quality issue of 119 slides (15%) which could interfere with interpretation. The majority of issues were related to immunostain slides and the most common defect was poor tissue detection of faint biopsy section on the slide (107/1610, 10%). We noticed abundant dark residue on reticulin slides (98/1610, 54%) resulting in an increase of scanned area, scanning time, and image file size. We also identified tracks of glue

on 18 slides (1%) which could contaminate the lens and result in blurred images and Venetian blind artifact. Other less significant issues were the inconsistent location of control tissue (14%), dirt (12%), control tissue out of coverslip (9%).

**Conclusions:** There is a high diagnostic concordance rate of WSI and LM of bone marrow core biopsy specimens. Improving histotechnology techniques could significantly affect the optimization of digital pathology for primary diagnosis. Continuous monitoring of image quality of different specimens is essential in learning the best histotechnology practices for a digital lab.

### **775 An Anatomical Pathology Digital Transformation Study in Preparation for Transition to a Fully Digital Laboratory Workflow**

Seow Ye Heng<sup>1</sup>, Ashley John<sup>2</sup>, Huimin Chua<sup>1</sup>, Jing Ning Hiew<sup>1</sup>, Patty Menghua Hsieh<sup>2</sup>, Chin Teck Kelvin Pow<sup>2</sup>, Angus Cameron<sup>2</sup>, Elena Lim<sup>2</sup>, Adeline Sng<sup>1</sup>, Chee Leong Cheng<sup>1</sup>

<sup>1</sup>Singapore General Hospital, Singapore, Singapore, <sup>2</sup>Philips Healthcare, Singapore, Singapore

**Disclosures:** Seow Ye Heng: None; Ashley John: None; Huimin Chua: None; Jing Ning Hiew: None; Patty Menghua Hsieh: None; Chin Teck Kelvin Pow: None; Angus Cameron: *Employee*, Philips Healthcare; Elena Lim: None; Adeline Sng: None; Chee Leong Cheng: None

**Background:** Improvements in digital pathology (DP) have been tremendous through the years and it is recognised that DP is playing an increasingly important role in diagnostic pathology. Our laboratory is looking into maximising benefits of DP with future full DP implementation in Anatomical Pathology. Some advantages of upfront digitalization of slide images includes seamless integration of future Artificial Intelligence intervention and ensuring business continuity via remote reporting in this current business climate. An end-to-end study of major workflows in the Histopathology laboratory was conducted, with an aim to consolidate current scanning benefits and projected benefits of full histopathology slide scanning. Time analysis comparing digital and analogue processes was performed on at least 25 work processes.

**Design:** To measure the potential benefits of a fully digital service, a Time and Motion study was performed. Firstly, the current and digital workflows in the Anatomical Pathology laboratory were mapped. Next, differences between analog and digital workflows, including impact to turnaround time (TAT), were identified. Following, 5 main processes comprising at least 25 sub-processes were evaluated and analysed. The 5 main processes were (i) Sort and Dispatch, (ii) Case Retrieval, (iii) Archival of slides, (iv) Multi-Disciplinary Tumour Board (MDT) and (v) Case Handling by pathologist. Each process was analyzed across multiple stakeholders, namely, pathologists, medical laboratory technologists (MLT), clerical coordinators and healthcare attendants (HCA).

**Results:** Total man-hour savings as a result of increase in efficiency due a digital workflow is 12,303 man hours per year. The main contributing factors to these savings were from the following 3 processes, Sort and Dispatch, Case Handling and MDT, where 4530, 4418 and 2385 man hours were saved per year, respectively. This figure translates into a 7% growth in capacity for the Anatomical Pathology department. With regard to process TAT, there is a 27% reduction in time required for "Sort and Dispatch" and 85% reduction in time for "Case Retrieval", which translates to potential consolidated reduction of 5800 hours per year.

**Conclusions:** Based on our Time & Motion study, and the differences between analog and digital processes, there is an opportunity for the Anatomical Pathology department to increase efficiency and accept additional case volume without affecting TAT whilst retaining the same headcount, through implementation of full DP.

### **776 Developing an Online Dashboard for Monitoring Cytopathology Workload**

Mohsen Hosseini<sup>1</sup>, Gavin Law<sup>2</sup>, Elham Khanafshar<sup>1</sup>

<sup>1</sup>University of California, San Francisco, San Francisco, CA, <sup>2</sup>UCSF Medical Center, San Francisco, CA

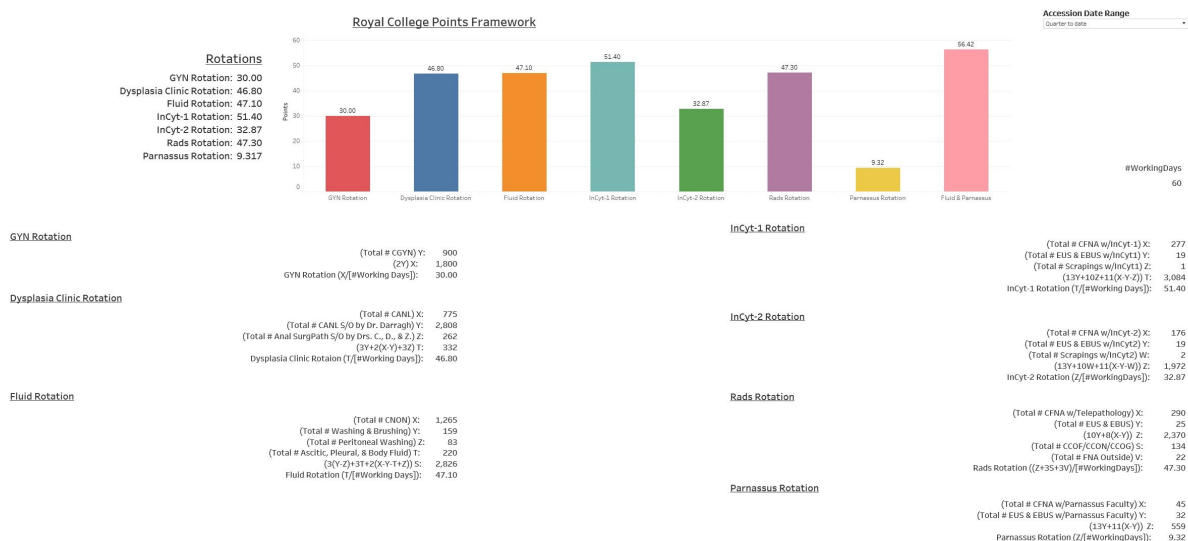
**Disclosures:** Mohsen Hosseini: None; Elham Khanafshar: None

**Background:** Accurate and fair measurement of workload is an ongoing challenge in pathology practices, essential to manage staffing and avoid burnouts. The Royal College of Pathologists (RCP) point system is a widely used system for evaluating workload. It has been shown to correlate with relative value units (RVU) while adjusting for the complexity of cases. Workload calculation is time-consuming which encumbers the implementation of the RCP point system. Here, we present our experience in developing an online dashboard for ongoing monitoring of RCP points. The dashboard facilitated equitable workload distribution and full-time equivalent (FTE) allocation in our practice.

**Design:** We designed a portal using dashboard feature of Tableau hosted on our institutional Tableau Webserver. The dashboard tracks workload by direct daily query of MS SQL database used by our lab information management system (LIMS), CoPath. The workload for each rotation is calculated from this data based on the RCP point system using case accession and rotation flags. Institutional holidays are provided by an external Excel calendar. Our design permits monitoring of workload over any specified time range and further customization.

**Results:** Our academic practice includes 15 pathologists, on 8 different rotations dispersed between three campuses. They perform case sign-out, fine-needle aspiration biopsies, and rapid on-site evaluations. To balance workload and determine FTE in this sophisticated practice, we implemented an annual RCP-based workload calculation in 2016. To be able to track dynamic changes in our practice, we have recently developed a dashboard to monitor RCP points for each rotation by direct query of our lab information management system (see design). The monitoring of RCP points for 2020 led to the merging of two of the rotations to equalize the workload and adjust faculty FTE.

Figure 1 - 776



**Conclusions:** RCP system provides an advanced system for evaluating workload. Optimal implementation of this system requires prospective allocation of points for each case which is time-consuming and often impractical. To address this issue, we have developed a dashboard for automated monitoring of points for each rotation. The portal has proved efficient in tracking RCP points for each rotation. We believe our experience is of benefit to other complex pathology practices who seek a dynamic system for workload evaluation and FTE allocation.

### 777 Web-Based Multi-Head Microscope with Alternating Driver Responsibility for Digital Pathology

Jeremy Jones<sup>1</sup>, Dibson Gondim<sup>2</sup>

<sup>1</sup>University of Louisville School of Medicine, Louisville, KY, <sup>2</sup>University of Louisville, Louisville, KY

**Disclosures:** Jeremy Jones: None; Dibson Gondim: None



**Background:** In the setting of “social distancing” during the COVID-19 pandemic, telepathology has become a critical topic. In some instances, microscope conferences with multiple participants, such as consensus conferences, have been moved from the multi-head microscope to live broadcast from microscope cameras of each individual participant. This format prevents the changeover of slide driving privileges to anyone viewing remotely. This limitation can be significant and may hinder the ability of consulting pathologists to providing a definitive opinion. Although slide scanners are available in some institution, not all digital pathology systems have a built-in application that allow multiple users to share slides seamlessly. The purpose of this project is to describe the creation and user-experience of a web-based digital slide viewer application that allow easy exchange of driving privileges between users. The web-application was created with open source technology.

**Design:** The back-end of the web-application was created with Python script using Flask framework. The front-end was created with HTML, javascript and CSS. Whole slides images were converted to Deep Zoom Image (DZI) file format and uploaded to a webserver. The DZI files are loaded in the webpage using the openseadragon javascript library. The web-application shows a list of participating users. This is updated in real time as users join and leave though use of Socke.IO javascript library, which sends data from one user to the server and back out to all users. A new driver can be selected from this list, which automatically unseats the old driver. The driver is able to move and magnify the slide using the openseadragon viewport which displays DZI files as a seamless array of image tiles. The driver’s x, y, and z coordinates are sent via Socket.IO to move and magnify the viewport of all other users. A pointer overlay also moves in unison with the driver’s mouse coordinates.

**Results:** The resulting application was launched using IBM Cloud Foundry. The URL for the application was shared with 6 pathology residents and faculty who were able to participate in a mock-interpretation of a slide. Throughout the exercise, 4 different users moved and changed the magnification of the slide for the group.

**Conclusions:** This application served as a working demonstration of how to integrate existing open source technologies to offer a multi head microscope experience over the web with the ability to alternate the slide driver.

### **778 Improved Detection of Acid-Fast Bacilli by Deep Learning Aided Digital Imaging**

Yuki Kanahori<sup>1</sup>, Yuka Kitamura<sup>1</sup>, Han-Seung Yoon<sup>2</sup>, Andrey Bychkov<sup>3</sup>, Junya Fukuoka<sup>1</sup>

<sup>1</sup>Nagasaki University, Nagasaki-shi, Japan, <sup>2</sup>Nagasaki University Hospital, Nagasaki-shi, Japan, <sup>3</sup>Kameda Medical Center, Kamogawa, Japan

**Disclosures:** Yuki Kanahori: None; Yuka Kitamura: *Stock Ownership*, N Lab Corp; Han-Seung Yoon: None; Andrey Bychkov: None; Junya Fukuoka: None

**Background:** Tuberculosis is among the leading infectious causes of morbidity and mortality worldwide. Microscopic detection of M. tuberculosis on the acid-fast stain is much time-consuming and reportedly produces false results. Recent advances in digital pathology prompted the transition from microscopes to digital diagnosis using whole slide images (WSI). However, recognition of mycobacteria on WSI is considered not efficient at this point. We evaluated if the use of a deep learning (DL) model can help improve the detection of mycobacteria in a WSI-based workflow.

**Design:** Two slides of autopsy cases with abundant acid-fast bacilli (AFB) and 40 slides of transbronchial lung biopsies (TBLB) known to be negative for mycobacteria were used for annotation and training. WSIs were scanned using extended focus mode (EasyScan 6, Motic). VGG model (Halo, Indica Labs) was used for DL training.

Forty-one TBLB specimens from patients radiologically suspected for tuberculosis and stained with Ziehl-Neelsen were enrolled in the study. Three pathologists evaluated the presence of bacilli with a microscope using a 40x objective lens, which reproduced a routine approach. Next, each pathologist accessed annotations produced by the DL model (appeared as highlighted areas when mycobacteria were detected by the algorithm) on WSI of the same cases and made judgment about AFB presence. The sensitivity and specificity of the two methods (microscope-based vs. DL-assisted) were calculated. A time spent by each pathologist for evaluating AFB with different methods was recorded.

The ground truth was obtained by consensus of the three pathologists by observing glass slides under a microscope with a 100x objective lens and oil immersion.

**Results:** Forty-six percent (19/41) of specimens contained AFB by the ground truth assessment. The sensitivities of the three pathologists to detect AFB with the microscope were 0.35, 0.47, and 0.06, and the specificity was 1.0, 0.87, and 1.0, respectively. With DL assistance, the sensitivity markedly increased to 0.94, 0.71, 0.35, and the specificity remained high at 0.83, 0.96, 0.78, by three pathologists, respectively. Furthermore, DL support decreased the observation time per specimen by almost 2.5x, from 1.31 minutes to 0.51 minutes.

**Conclusions:** Our data suggest that the use of DL improves the detection of mycobacteria by increasing sensitivity and saving time.

## **779 Usage Analysis and Performance Assessment of a Home-Brewed Java-Based Anatomic Pathology Diagnosis Search Program Based on Complete Vocabulary Indexing**

Kyungmin Ko<sup>1</sup>, Robert Miller<sup>2</sup>

<sup>1</sup>MedStar Georgetown University Hospital, Alexandria, VA, <sup>2</sup>Johns Hopkins Medicine, Baltimore, MD

**Disclosures:** Kyungmin Ko: None; Robert Miller: None

**Background:** When pathology residents preview slides, they look up similar cases from the past to see how they were phrased and what features were important. To overcome limitations in speed and convenience of the department's existing Laboratory Information System, I developed an application, the Anatomic Pathology Diagnosis Search (APD). I analyzed the usage logs to understand how ADPS has been adopted by the Department and to optimize the search algorithm.

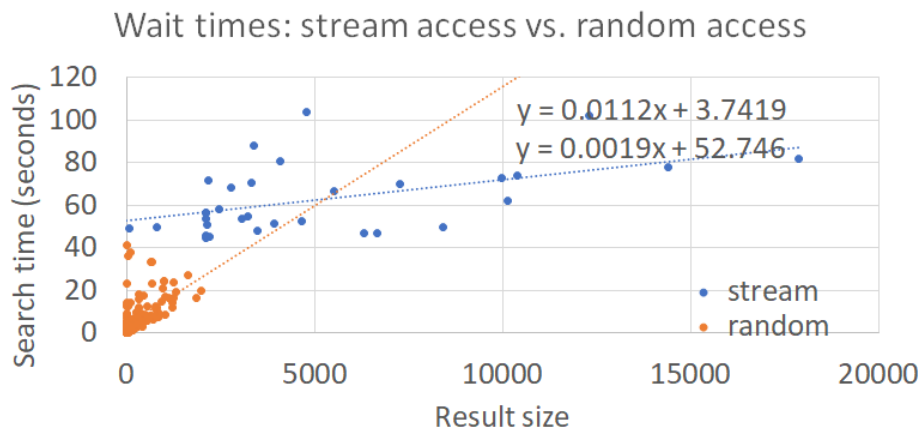
**Design:** A Java .jar application was developed using Open JDK 8.0. The program and underlying database file is located on the departmental shared network drive with access controls for departmental access. The program is launched from any of the hospital's workstations by users with read permissions on the Pathology department drive. It requires a Java Virtual Machine, which is already installed on most of the hospital's workstations. The custom-built database contains departmental surgical pathology diagnoses from 2009 to present. Notable algorithmic details are 1) complete indexing of all terms (Figure 2), and 2) switching between stream based and random access of the database. I logged every search job performed from October 7 to December 10, 2019 and analyzed the log.

**Results:** On an average weekday,  $19 \pm 15$  (mean  $\pm$  SD) search jobs were performed, evidencing avid adoption of this tool by the Pathology Department. The most frequently searched term was "placenta" (Table 1). 'Adenocarcinoma' was the next most frequently searched keyword (12 times) tool, but it was seldom the first search term used.(2 times), indicating users utilized the strategy of searching with a more specific keyword before a less specific one.

The program was primarily used by residents on preview duty to use previous reports as templates to draft new reports. It also found rare cases for research purposes, which were previously impossible to find (anecdotal). The median wait time for search results were 1.43 seconds overall, 1.77 seconds for first searches, and 0.46 seconds for searching within search results. The database contains approximately 110,000 cases and occupies only 437 megabytes on disk as of February 2020. From preliminary data it was apparent that when the database was accessed as a random-access file, the wait time increased linearly in relation to the result count. During the data collection interval, the program was set to access the entire database as a stream if an index lookup found more than 2000 entries. This occurred 32 times, resulting in relatively stable wait times of 49.7 to 71.7. The wait time for random access was more variable and subject to network latency and exceed the wait time of stream reading when results exceed approximately 5000 cases.

Search phrases by frequency		
	Number of searches	
	Total	As first phrase
"placenta"	16	13
"adenocarcinoma"	12	2
"amputation"	11	10
"breast"	10	3
"liver"	9	4
"hepatic adenoma"	8	8
"Whipple"	8	7
"ampulla"	7	7

Figure 1 - 779



**Conclusions:** ADPS implements full vocabulary indexing and switching between file access modes for an excellent search experience. It was successfully deployed into daily surgical pathology workflow and now highly utilized.

**780 Sources of Scan Failure in a High-Throughput Slide-Scanning Facility**

Mark Lloyd<sup>1</sup>, David Kellough<sup>1</sup>, Trina Shanks<sup>1</sup>, Molly Flynn<sup>1</sup>, Anil Parwani<sup>2</sup>  
<sup>1</sup>Inspirata, Inc., Tampa, FL, <sup>2</sup>The Ohio State University, Columbus, OH

**Disclosures:** Mark Lloyd: *Employee*, Inspirata, Inc.; David Kellough: *Employee*, Inspirata; Trina Shanks: *None*; Molly Flynn: *None*; Anil Parwani: *None*

**Background:** In a digital pathology work flow, scan errors and failures mean delays to patient diagnosis and treatment. Delays mean unhappy clinicians and administrators. While uncommon (just 1.22% of the 1,687,289 slides we have scanned), even a small percentage of a very large number has the potential to cause havoc. Scan failures might become less common still if we are able to ascertain the sources of slide scan failure and how we might intervene.

**Design:** For the month of September 2020 (21 business days), we monitored scanner errors, noting—if possible—the likely cause. Error reports came to us through scanner reports of failed scans (failed ROI detections, slides skipped, slides dropped, tissue not detected, and other faults), scan tech visual inspection of 100% of images for correct ROI, intensive review of 1.5% of all slides scanned, and pathologist reports of problem scans. Judgement of scan fail cause was based on the inspection of the slides by National Society for Histology-certified scan techs drawing on their years of experience in a high-throughput slide scanning facility producing over 500,000 whole slide images a year.

**Results:** In September 2020, we scanned 43,756 slides. We encountered 532 errors amounting to 1.22% of the total volume scanned. Breakdown of errors and their assignment to cause is as follows:

The vast majority of scan failures (89%) are attributable to scanner issues.

Error	TOTAL	Machine Error	Slide Prep	Unknown
ROI	421	421	0	0
Tissue Skipped	55	55	0	0
Other	22	0	0	22
OOF	21	0	21	0
Slide Dropped	13	0	13	0
<b>TOTAL</b>	<b>532</b>	<b>476</b>	<b>34</b>	<b>22</b>

**Conclusions:** For most slide errors the answer is in the hands of scanner manufacturers and software designers.

Scan failures can, however, be reduced by careful slide preparation. The IT aphorism GIGO—garbage in, garbage out—applies equally to slide scanning. Many scan fails are attributable to features of the slide. Misaligned coverslips and badly applied labels are typically to blame for dropped slides. Out-of-focus slides have a variety of avoidable causes. Markings on the coverslip, debris or fingerprints on the coverslip, excess mounting media at the edge of the coverslip, poor histology, wrinkled or folded tissue, and tissue of variable thickness can all cause a slide image to be out-of-focus.

**781 The Use of a Novel Digital Tumor Board Platform Reduces Pathologist Tumor Board Preparation Time and Enhances Clinician Satisfaction: the UCLA Experience**

Alexander Nobori<sup>1</sup>, Chayanit Jumniensuk<sup>1</sup>, Shawn Chen<sup>1</sup>, Sarah Dry<sup>2</sup>, Scott Nelson<sup>2</sup>, Corey Arnold<sup>1</sup>  
<sup>1</sup>David Geffen School of Medicine at UCLA, Los Angeles, CA, <sup>2</sup>University of California, Los Angeles, Los Angeles, CA

**Disclosures:** Alexander Nobori: None; Chayanit Jumniensuk: None; Shawn Chen: None; Sarah Dry: None; Scott Nelson: None; Corey Arnold: None

**Background:** Multi-disciplinary oncology meetings, or tumor boards, are held to improve communication between specialties regarding the management of complex cancer cases and to provide improved patient care. We developed a novel digital platform to increase the efficiency of tumor board preparation, reduce errors in patient entry, and provide enhanced communication to the clinical team.

**Design:** During a prospective, consecutive seven-week period, pathology preparation for the weekly musculoskeletal tumor board was performed using the conventional method and the digital platform by two pathology fellows. The preparation time for each method was measured. In the conventional method of patient submission to the tumor board list, patient entry errors were recorded. These errors were recorded again after implementation of the digital platform for patient entry. Participating clinicians and radiologists completed a survey evaluating satisfaction with the digital platform.

**Results:** Tumor board preparation was performed for 159 patients using both the conventional and digital methods for seven tumor board meetings. Preparation of tumor board using the digital tumor board platform showed a 45% reduction in time compared to the conventional method over the seven-week study interval. A two-sided Wilcoxon rank sum test demonstrated that the median preparation time using the digital platform was significantly lower than the median preparation time for the conventional method ( $p < 0.01$ ) at an alpha level of 0.05. Three patient-entry errors were observed in the pre-implementation period and none were observed in the post-implementation period. A survey of participating clinicians and radiologists showed 91% preferred the digital method over the conventional method.

Figure 1 - 781

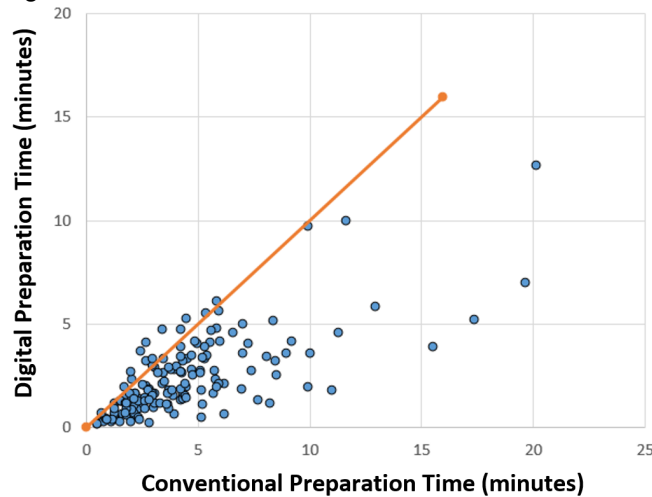


**Figure 1.** Preparation time in the conventional and digital methods for each of the 159 patients.

**Conclusions:** Use of a novel digital tumor board platform resulted in significant reduction in preparation time for pathologists, reduction of patient entry errors, and improved clinician and radiologist satisfaction with pathology presentation.

**782 Deep Neural Networks Can Facilitate Diagnosis and Histologic Classification of Renal Cell Carcinoma on Biopsy and Surgical Resection Slides**

Ryland Richards<sup>1</sup>, Mengdan Zhu<sup>2</sup>, Naofumi Tomita<sup>2</sup>, Matthew Suriawinata<sup>2</sup>, Saeed Hassanpour<sup>2</sup>, Bing Ren<sup>1</sup>  
<sup>1</sup>Dartmouth-Hitchcock Medical Center, Lebanon, NH, <sup>2</sup>Dartmouth Geisel School of Medicine, Hanover, NH

**Disclosures:** Ryland Richards: None; Mengdan Zhu: None; Naofumi Tomita: None; Matthew Suriawinata: None; Saeed Hassanpour: None; Bing Ren: None

**Background:** The accurate classification of renal cell carcinoma (RCC) into the correct subtype is a vital component of pathologic diagnosis of these tumors. This task is challenging due to morphologic similarities between subtypes, and it can be even more difficult in biopsy specimens, as there may be limited tumor tissue available for histologic examination or immunohistochemical staining. As imaging-guided biopsy technologies continue to improve, pathologists may be more frequently expected to make this diagnosis on needle biopsy samples. In this study we trained a convolutional neural network (CNN) to detect and differentiate between three subtypes of RCCs (clear cell, chromophobe, and papillary), as well as oncocytoma and normal kidney, using whole slide images of surgical resection slides. We then applied this model to resection slide test sets and a biopsy slide test set.

**Design:** Whole slide images from renal mass resection specimens at our institution (n = 408) were annotated by pathologists for regions of interest and used to train a CNN, which was then applied to a test set of 78 resection slides as well as a set of 79 biopsy slides. External validation was performed with 69 whole slide images of renal cancers from the Cancer Genome Atlas (TCGA). The CNN used deep neural network image analysis to make predictions based on small, fixed-size patches, then pooled the predictions together to generate a final classification for each slide. Performance was assessed by calculating precision, recall, accuracy, and F1 score.

**Results:** The CNN model achieved high performance for histologic classification on the internal resection test set, biopsy test set, and external validation set with mean accuracy of 0.97, 0.97 and 0.98, mean precision 0.94, 0.97 and 0.97, mean recall 0.92, 0.93 and 0.95, and mean FI-score 0.92, 0.95 and 0.96, respectively. The average area under the curve (AUC) on the internal resection set, internal biopsy set, and external validation set was 0.98, 0.98 and 0.99, respectively. Whole-slide image patch visualization revealed specific morphologic features that led to misclassification, and confusion matrices illuminated which diagnoses had been made in error.

**Conclusions:** We developed a deep learning network to accurately detect and differentiate between three subtypes of RCC, as well as oncocytoma and normal kidney, when applied to whole slide images. Our model performed well on both resection and biopsy slide sets, indicating its potential for aiding pathologists to make diagnoses in challenging cases or when limited tissue is available. To our knowledge, this is the first application of a deep learning network to the detection of RCC and oncocytoma on renal biopsy slide images. Future directions will include assessing how the use of this model will affect pathologists' efficiency and accuracy in diagnosing renal masses.

**783 Direct Electronic Reporting of Frozen Section Results With a Novel Web-based Software Program - A Paperless Alternative to Traditional Frozen Section Workflow**

Jon Ritter<sup>1</sup>, Joseph Gaut<sup>2</sup>, Hannah Krigman<sup>1</sup>, Jared Amann-Stewart<sup>1</sup>, Jonathan Bihr<sup>2</sup>, Greg Robbins<sup>2</sup>, Lulu Sun<sup>3</sup>, H. Michael Isaacs<sup>2</sup>

<sup>1</sup>Washington University School of Medicine, St. Louis, MO, <sup>2</sup>Washington University in St. Louis, St. Louis, MO, <sup>3</sup>Washington University School of Medicine in St. Louis, St. Louis, MO

**Disclosures:** Jon Ritter: None; Joseph Gaut: None; Hannah Krigman: None; Jared Amann-Stewart: None; Jonathan Bihr: None; Greg Robbins: None

**Background:** Our existing frozen section workflow included handwritten reports, communicated to the operating room (OR) via speaker phone. We believe this is a patient safety issue, with the opportunity for misinterpretation of verbal reports. The paper workflow also requires rework in the form of dictation of handwritten diagnoses, with potential errors. In addition, generation of turnaround data required manual review of paper logs which were often not completed, or were unreliable. Finally, with use of telepathology for remote frozen section locations, it was difficult to use a paper workflow where the paper needed to follow the specimen at locations remote from where the paper reports would be generated.

**Design:** To address these concerns, we developed a web-based software platform with a bidirectional interface with our laboratory information system (LIS) - Cerner CoPath Plus. Inspired by a similar system developed at Yale University, this software was written at Washington University, in .NET, and runs on a sql server. It is password protected, and HIPAA-compliant. Accessioning of a frozen section in the LIS opens the case in the frozen section module where diagnosis entry occurs. Because this work occurs outside of the LIS, the case is not locked in the LIS, and additional frozen section parts can be accessioned into the LIS simultaneously with work occurring in the module. Signout of the frozen in the module software then writes the diagnosis directly into the intraoperative consult section of CoPath, and also sends the information directly to the operating room, where it can be read and acknowledged by the operating room staff. Other software features include links to open digital scanned images for telepathology directly through the module. A link can display gross images to a remote pathologist, and also share gross images with the OR for gross consults. There are also links to open prior cases in the LIS for review with the current case.

**Results:** The process has been in use in the Pathology laboratory for 6 months, and has streamlined entry of frozen section results and gross consultations into the LIS. In particular pathologist assistants and residents have expressed satisfaction at the time savings generated by not having to re-dictate hand-written frozen section and gross consult reports. Ease and accuracy of turn-around time computations have been enhanced by this software solution. In addition, this system facilitates transmission of results for frozen sections performed by telepathology. The OR portion of the software has cues to highlight already signed out results, cases awaiting OR acknowledgement, and cases in process in the Pathology laboratory.

**Conclusions:** An electronic frozen section reporting system can improve patient safety, will enhance assessment of quality metrics, can streamline workflows, and also allows for ease of reporting from remote locations for telepathology.

**784 Collaborative Workflow Between Pathologists and Deep Learning Model to Improve Tumor Cellularity Counts**

Taro Sakamoto<sup>1</sup>, Tomoi Furukawa<sup>1</sup>, Satoshi Yoshida<sup>2</sup>, Yukio Kashima<sup>3</sup>, Kurumi Seki<sup>2</sup>, Andrey Bychkov<sup>2</sup>, Junya Fukuoka<sup>4</sup>

<sup>1</sup>Nagasaki University, Nagasaki, Japan, <sup>2</sup>Kameda Medical Center, Kamogawa, Japan, <sup>3</sup>Awaji Medical Center, Awaji, Japan, <sup>4</sup>Nagasaki University, Nagasaki-shi, Japan

**Disclosures:** Taro Sakamoto: None; Tomoi Furukawa: None; Satoshi Yoshida: None; Yukio Kashima: None; Kurumi Seki: None; Andrey Bychkov: None; Junya Fukuoka: None

**Background:** Due to high demand of molecular testing, reporting tumor cellularity in cancer samples becomes a mandatory task for pathologists. However, its estimation by pathologists has been reported inaccurate. To improve this issue, we built a collaborative workflow between pathologists and artificial intelligence (AI) models to evaluate tumor cellularity in lung cancer samples and applied it to routine practice prospectively.

**Design:** As reported previously, deep convolutional neural network model and image analysis to efficiently evaluate tumor area and nuclear count were constructed, respectively. In short, VGG (HALO AI®, Indica Lab) was trained and validated using annotated 50 cases of lung adenocarcinoma transbronchial biopsy samples, and applied it prospectively to measure tumor cellularity in lung adenocarcinoma samples collected from 3 institutes of our digital diagnostic network from April 2019 to September 2020.

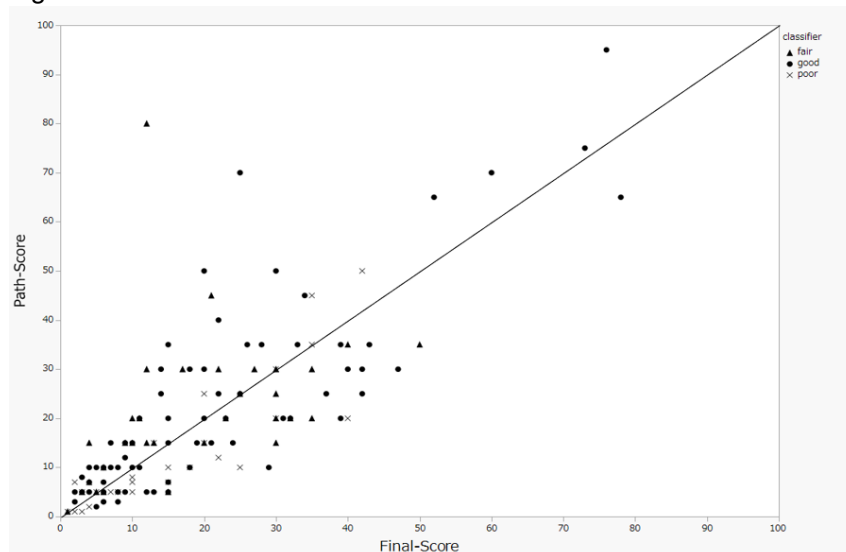
The workflow was set as follows. 1)whole slide images of adenocarcinoma cases were immediately transferred to AI analysis. 2)Evaluated results were shared at sign out sessions on the next business day. 3)Pathologists estimated tumor cellularity (Path-Score), the percentage of tumor cells in total cells. 4)Pathologists reviewed the results of AI analysis (AI-Score). 5)The pathologists determined the final percentage (Final-Score) with modification to AI-Score. We also judged the quality of AI analysis into 3 levels; good (>90% accuracy), fair (>50% accuracy), and poor.

**Results:** Total of 151 lung adenocarcinoma cases, 85 TBB (transbronchial biopsy), 38 CNB (core needle biopsy), 15 TBNA (transbronchial needle aspiration), 7 surgical specimens, and 6 cell blocks were prepared for test case and analyzed. Among them, 80 cases (53%), 38 cases (25%), and 33 cases (22%) were judged as good, fair, and poor, respectively.

One pathologist attending all sign outs met change in 132 cases (87.4%) from his initial Path-Score (Figure 1). This result indicates that pathologists reconsidered their impression after referring to data of AI and illustrates a good model of a collaboration between pathologists and AI to improve practice.

The initial pathologist's impression improved gradually and stabilized after experience of approximately 30 cases. Among tested modalities, TBNA/TBAC met the highest rate, 93%, of good judgement compared to others.

Figure 1 - 784



**Conclusions:** We have successfully implemented AI into routine practice. Our model of tumor cell count efficiently supports pathologists to improve prediction of tumor cellularity for genetic tests.

**785 The New Kid on the Block – Implementation of the Newly FDA-Cleared Scopio Labs™ X100 with Full Field Peripheral Blood Smear Application for Research and Training During the COVID-19 Pandemic**

Christian Salib<sup>1</sup>, Mehrvash Haghighi<sup>2</sup>, Eileen Scigliano<sup>1</sup>, Julie Teruya-Feldstein<sup>3</sup>

<sup>1</sup>Icahn School of Medicine at Mount Sinai, New York, NY, <sup>2</sup>Mount Sinai Hospital, New York, NY, <sup>3</sup>Mount Sinai Hospital Icahn School of Medicine, New York, NY

**Disclosures:** Christian Salib: None; Mehrvash Haghighi: None; Eileen Scigliano: None; Julie Teruya-Feldstein: None

**Background:** Digital pathology and artificial intelligence (AI) is a popular and rapidly growing field of Pathology. A growing number of institutes have integrated digital imaging into routine workflow, relying on AI algorithms for the detection of prostate cancer, mitotic figure enumeration and evaluating degree of glomerular disease. Despite advances and increased use of Whole Slide Imaging (WSI) for tissue evaluation, the field of Hematopathology and Cytology has lagged behind other subspecialties. Moreover, during the current Sars-CoV-2 (COVID-19) pandemic, social distancing and contact precautions have posed challenges in colleague interaction, specimen handling and processing, resulting in overall segregations between healthcare colleagues. We implemented a new Scopio Labs X100 digital imaging instrument, which provides high resolution oil-immersion level images of large scanned areas. Most striking is its ability to clearly and accurately detect single cells in body fluid smears with high fidelity. To the best of our knowledge, we are first among a handful of institutions to implement the Scopio Labs X100 digital slide imaging for bone marrow aspirates (BMA), cytology and peripheral blood smears (PBS) for research and training purposes.

**Design:** Data obtained was covered under an IRB waiver, HS#:12-00133 GCO#1:12-036(0001-08). Representative PBS, BMA and cytology fluid smears were digitized and catalogued with Scopio Labs X100 Full Field Digital scanner. Scanned images were evaluated by Pathologists, Hematologists and medical trainees. To complement our Philips™ Whole Slide Imaging system, consult cases with bone marrow biopsies, lymph node and extranodal tissues were also scanned with Scopio instrument for archival purposes.

**Results:** 414 cases and representative slides were digitized at 100x magnification over 6 months duration, including PBS, BMA and cytology specimens (**Figure 1**). Various entities have been identified, including, acute myelomonocytic leukemia (AMML), hypersegmented neutrophils in COVID-19(+) patients, myelodysplastic



syndrome (MDS), metastatic disease and COVID-19-related neutrophil hypersegmentation & atypical lymphocytes (Figure 2). Study sets for PBS were created for training purposes, including hemoglobinopathies, lymphoproliferative neoplasms and myelodysplastic changes.

Figure 1 - 785

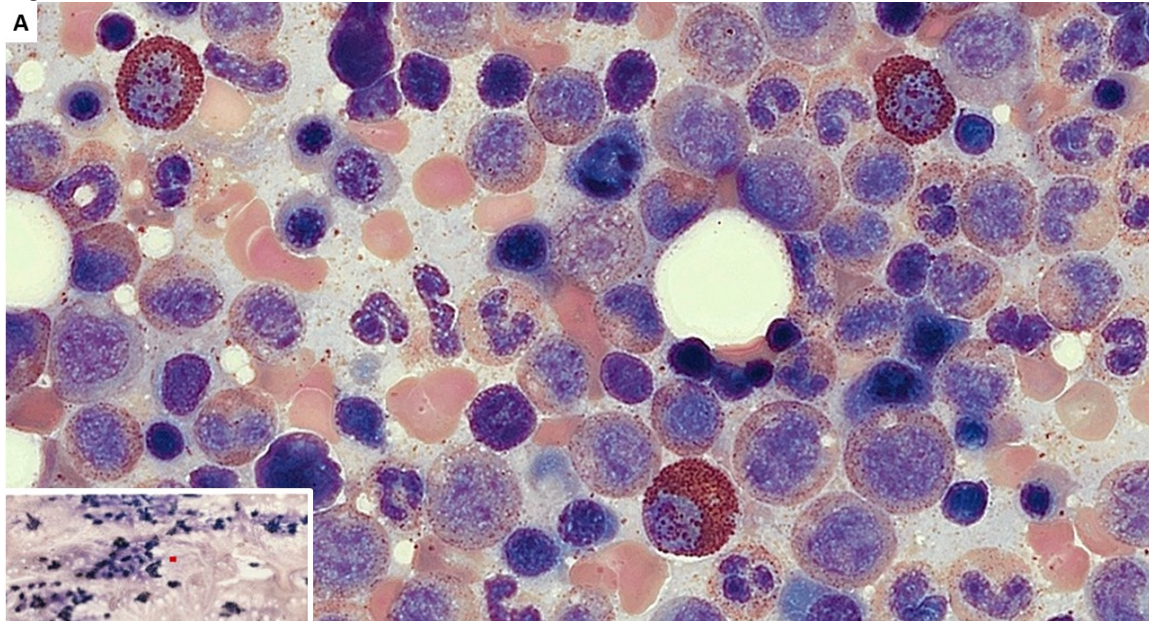


Figure 1. Digitized bone marrow aspirate smear at 100X (inset showing overall smear quality with red square showing area of focus)

Figure 2 - 785

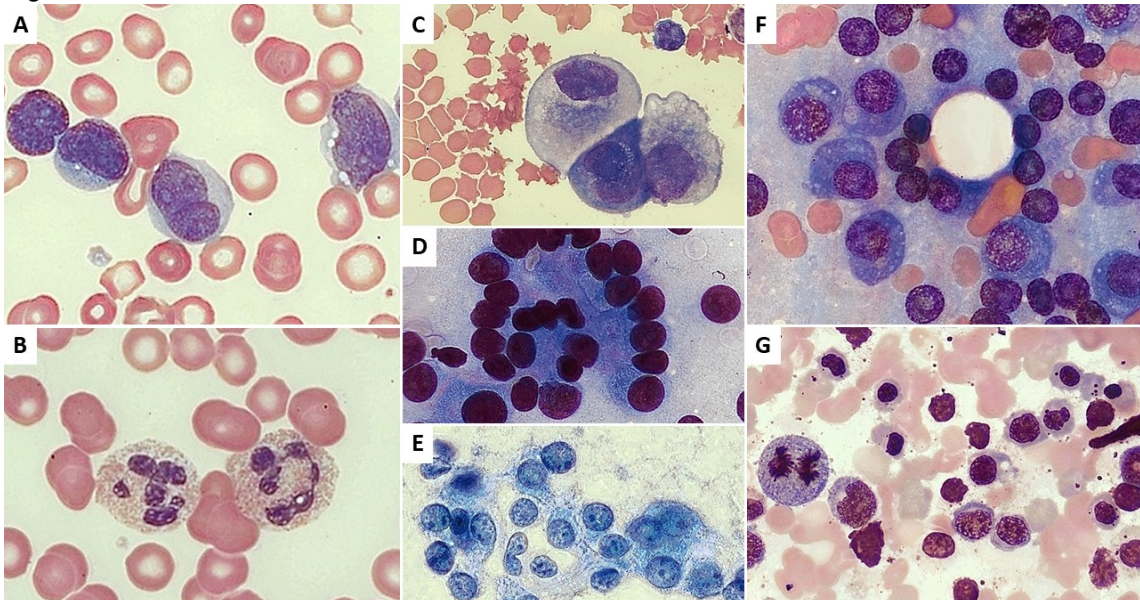


Figure 2. Various fluid smear images captured at 100X magnification, including AMML (A) and hypersegmented neutrophils from a COVID-19(+) patient (B) in peripheral blood, mesothelial cells with acanthocytes on peritoneal fluid cytopsin (C), cytology fluid slides with Diff Quik (D) and PAP stain (E), and plasma cell myeloma (F) and dyserythropoiesis (G) on bone marrow aspirates

**Conclusions:** The Scopio Labs X100 digital system provides an accurate, efficient and timely web-based digital tool and image bank to accommodate the social distancing challenges during the COVID-19 pandemic for Hematology, Hematopathology and Cytopathology medical students, clinical Hematology/Oncology and Pathology trainees. With its recent FDA-clearance, we aim to fully integrate Scopio Labs into our LIS and assess the full field PBS application to streamline our workflow.

**786 Tumor Fraction Estimation to Assess Copy Number Alterations and Germline Mutations in a Next Generation Sequencing Panel**

Stephanie Siegmund<sup>1</sup>, Fei Dong<sup>1</sup>  
<sup>1</sup>Brigham and Women's Hospital, Boston, MA

**Disclosures:** Stephanie Siegmund: None; Fei Dong: None

**Background:** Pre-analytical surgical pathological evaluation, including estimation of tumor fraction, is critical to the interpretation of cancer panel next generation sequencing (NGS) results. Tumor fraction influences variant calling of somatic mutations and copy number estimation, particularly in the setting of unpaired tumor sequencing where no background normal tissue sample is available for comparison. However, tumor fraction estimation is not routinely performed in most cancer NGS pipelines.

**Design:** We develop a framework for estimating tumor fraction from NGS sequencing data by evaluation of copy number neutral and one-copy deletion states. Tumor fraction is validated by comparison with colorectal adenocarcinomas with pathogenic RAS pathway gene mutations. We then apply the methodology to determine absolute copy number estimation for *ERBB2* in breast carcinomas. We then apply the methodology in breast carcinomas to determine absolute copy number estimation for *ERBB2* and germline status for *BRCA1* and *BRCA2* mutations.

**Results:** In 125 cancers, the calculated tumor fraction based on our approach was positively associated with visual estimation by histopathology. Histological estimations were within 10% of calculated tumor cellularity in 45% of specimens (n=56) and within 20% of calculated tumor cellularity in 73% of specimens (n=91). In 14 colorectal cancers with *KRAS*, *NRAS*, or *BRAF* mutations, the driver mutation allele fraction was more strongly correlated with calculated tumor fraction ( $R^2=0.51$ ) compared with histopathologic estimation ( $R^2=0.16$ ). In 13 breast carcinomas with equivocal HER2 staining by immunohistochemistry, absolute *ERBB2* copy number estimation by sequencing was strongly correlated with manual counts by fluorescence in situ hybridization ( $R^2=0.86$ ). In 17 patients with known pathogenic *BRCA1* or *BRCA2* germline variants, tumor only sequencing data accurately estimated that non-neoplastic cells in the specimen contained a mean of 1.06 copies of the pathogenic variant per cell (standard deviation 0.24 copies).

**Conclusions:** Here, we demonstrate that tumor fraction can be inferred from next generation sequencing data. This method can in turn be utilized to improve quantitative copy number analysis and evaluate germline status in clinical sequencing specimens.

**787 Building an Integrative Multi-Omic Pathology Biorepository Research Database**

Joachim Silber<sup>1</sup>, Ming Yang<sup>1</sup>, Maria Corazon Mariano<sup>1</sup>, Shai Ahmed<sup>1</sup>, Umesh Bhanot<sup>1</sup>, Faruk Erdem Kombak<sup>1</sup>, Lorraine Corsale<sup>1</sup>, Lev Sipershteyn<sup>1</sup>, Kai-Hsiung Lin<sup>1</sup>, Stuart Gardos<sup>1</sup>, Michael Roehrl<sup>1</sup>  
<sup>1</sup>Memorial Sloan Kettering Cancer Center, New York, NY

**Disclosures:** Joachim Silber: None; Ming Yang: None; Maria Corazon Mariano: None; Shai Ahmed: None; Umesh Bhanot: None; Faruk Erdem Kombak: None; Lorraine Corsale: None; Lev Sipershteyn: None; Kai-Hsiung Lin: None; Stuart Gardos: None; Michael Roehrl: None

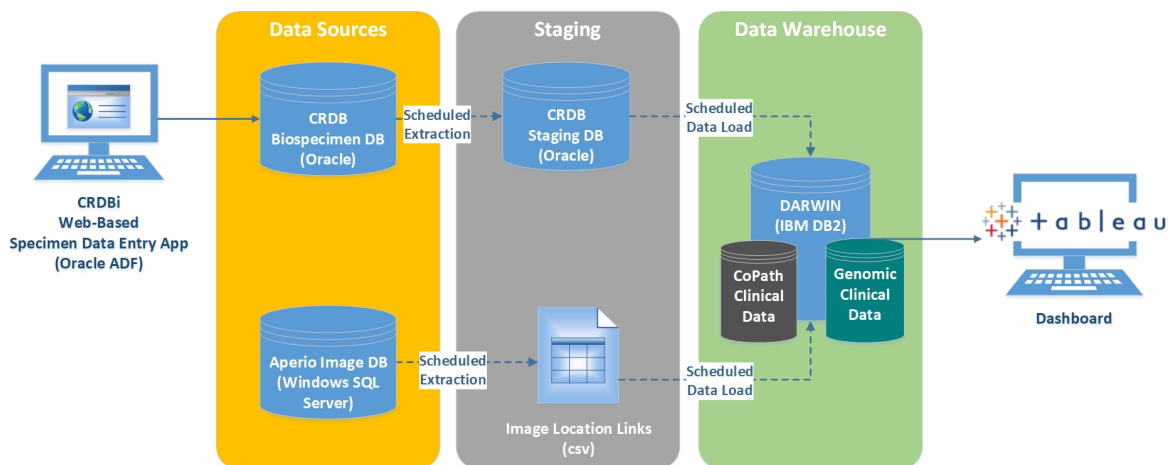
**Background:** The Biobank of the Precision Pathology Biobanking Center (PPBC) at Memorial Sloan Kettering Cancer Center (MSK) collects research specimens from >6,000 new cancer patients per year. Biospecimen data (e.g. physical location, unit type, processing time, etc.) is entered into an in-house Oracle database – CRDB (Clinical Research Database). We recently built data pipelines around CRDB to produce more valuable data visualization and analysis. Here, we present our attempt at linking frozen pathology research specimen data with digital pathology images, genomic data, and CoPath data by leveraging MSK's data warehouse.

**Design:** The MSK Darwin database is an enterprise data warehouse (IBM DB2 LUW) containing demographic, clinical, and genomic data from various upstream sources including PPBC's biorepository data. Newly procured

biospecimen data is extracted and transferred daily from CRDB to Darwin. Digital hematoxylin and eosin slides (H&Es) are prepared from spatially indexed research formalin-fixed and paraffin-embedded (FFPE) blocks that match each sampling location of a corresponding frozen vial. All samples and slides are barcoded, and relevant image data is uploaded to the Darwin database using a python script extracting pertinent data from the Leica Aperio eSlide Manager, which is stored inside a Windows SQL server.

**Results:** Detailed Tableau dashboards, integrating data from Darwin, allow biobank users to carry out complex queries on various patient data (PHI, demographics, consent status, etc.), biospecimen data (distribution status, ischemic time, physical location, etc.), and corresponding digital H&Es. By centralizing data visualization in Tableau, the need to log into multiple siloed data systems has been reduced. Our integrative system links frozen research biospecimens with >38,000 digital H&Es (digitization started in 2017) and with clinical genomic data on >12,000 cases. Overall, our research biobank database includes >500,000 sample units from >125,000 processed cases over >25 years.

Figure 1 - 787



**Conclusions:** Our platform (Figure 1) is a powerful information management system that brings together information from disparate locations to enable users to effectively address data silo challenges. It is a highly configurable informatics platform that is designed to facilitate and optimize research use of pathology tissue samples. Integrating digital H&Es with the physical biorepository allows users to evaluate frozen biospecimens without the need to thaw the samples.

**788 Whole Slide Imaging of Peripheral Blood Smears for Diagnostic Purposes**

Jacob Spector<sup>1</sup>, Lucy Han<sup>1</sup>, Joanna Balcerek<sup>1</sup>, Marietya Lauw<sup>1</sup>, Parul Bhargava<sup>1</sup>, Laura Brown<sup>1</sup>, Kristie White<sup>1</sup>, Scott Kogan<sup>1</sup>, Linlin Wang<sup>1</sup>

<sup>1</sup>University of California, San Francisco, San Francisco, CA

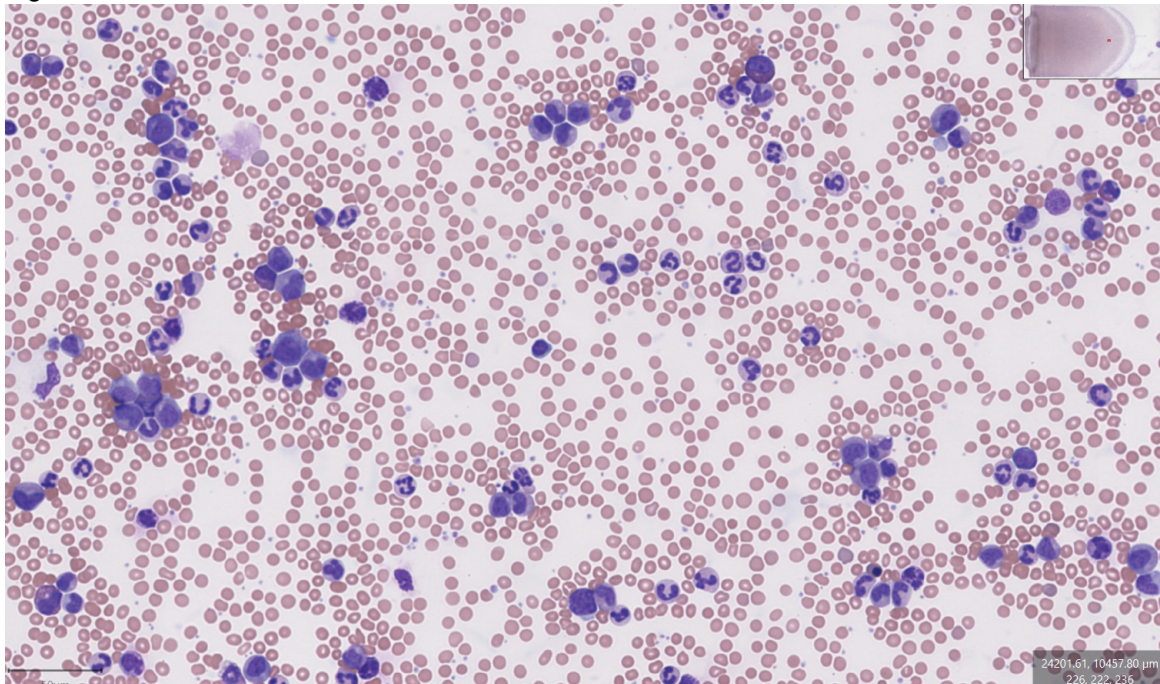
**Disclosures:** Jacob Spector: None; Lucy Han: None; Joanna Balcerek: None; Marietya Lauw: None; Parul Bhargava: None; Laura Brown: None; Kristie White: None; Scott Kogan: None; Linlin Wang: None

**Background:** Digital pathology is increasingly being used as part of clinical practice, especially in the setting of the COVID19 pandemic. Many institutions have begun incorporating Whole Slide Images (WSIs) into surgical pathology services; however, hematopathology faces additional technical limitations, such as higher magnification and cells located in different focal planes. Cellavision software can be used to aid in peripheral blood smear (PBS) review, but a definitive diagnosis may not be reached by using Cellavision alone. Here we examine scanned PBSs to evaluate the feasibility of using WSIs as part of clinical hematology sign out.

**Design:** A total of 96 PBS slides referred for pathologist review from 8/2020-10/2020 were collected and then scanned at 40x using an Aperio AT2 slide scanner. Diagnoses for these cases were first made by hematopathologists using standard clinical workflows and light microscopy. Digital slides were independently reviewed by at least one of two additional pathologists using Aperio Image Scope or QuPath software. The diagnosis based on digital slide review was recorded and compared to the original diagnosis.

**Results:** The major referral reasons included increased schistocytes, rare blasts, increased blasts, more than 10% immature granulocytes, reactive lymphocytes, abnormal lymphocytes, dysplastic neutrophils, or hypersegmented neutrophils. Of the 96 total cases examined 23 had significant red cell findings, 74 had significant white cell findings, and 2 had significant platelet findings. Among the cases with white cell findings, 31 were malignant. No diagnostic discrepancies were identified between digital slide review and light microscope review. Significant diagnoses included microangiopathic hemolytic anemia (3), acute leukemia (13, including AML with monocytic differentiation [4] and pediatric ALL [1]), lymphoproliferative disorder (7), chronic myeloid leukemia (3) (Figure 1, digital image), therapy related myeloid neoplasm (3), plasma cell neoplasm (2), other myeloid neoplasm (4), and transient abnormal myelopoiesis associated with Down syndrome (1). Of the 36 cases with blasts identified, 22 (61%) were malignant, 10 (28%) were reactive, and 4 (11%) had uncertain clinical significance. Important benign diagnoses included reactive lymphocytosis (6) and pseudo-Pelger-Huët anomaly (4). Compared to light microscope review, digital slide review was slower due to loading time for opening slide files and changing magnification. Twenty-two (24%) slides had to be rescanned because they were out of focus or had scanning artifacts.

Figure 1 - 788



**Conclusions:** Based on our findings, there is strong concordance between slide-based and WSI-based diagnoses for PBSs and we believe that it is possible to incorporate PBS WSIs into clinical workflows. To complete our clinical evaluation, we will collect additional cases with promonocytes to further confirm our findings.

**789 Characterizing Spatial Patterns of Immune Response in H&E Images from COVID-19 and H1N1 Autopsies Using Digital Pathology**

Paula Toro<sup>1</sup>, German Corredor<sup>1</sup>, Kaustav Bera<sup>1</sup>, Dylan Rasmussen<sup>1</sup>, Edana Stroberg<sup>2</sup>, Lisa Barton<sup>2</sup>, Eric Duval<sup>2</sup>, Hannah Gilmore<sup>3</sup>, Sanjay Mukhopadhyay<sup>4</sup>, Anant Madabhushi<sup>1</sup>

<sup>1</sup>Case Western Reserve University, Cleveland, OH, <sup>2</sup>Office of the Chief Medical Examiner, Oklahoma City, OK, <sup>3</sup>University Hospitals Case Medical Center, Case Western Reserve University, Cleveland, OH, <sup>4</sup>Cleveland Clinic, Cleveland, OH

**Disclosures:** Paula Toro: None; German Corredor: None; Kaustav Bera: None; Dylan Rasmussen: None; Edana Stroberg: None; Lisa Barton: None; Eric Duval: None; Hannah Gilmore: None; Sanjay Mukhopadhyay: None; Anant Madabhushi: *Advisory Board Member, Aiforia Inc; Primary Investigator, Bristol Myers-Squibb; Primary Investigator, AstraZeneca; Primary Investigator, Boehringer-Ingelheim*

**Background:** Computational pathology approaches offer the opportunity for quantitatively capturing and describing immune patterns in digitized pathology images. In this study, we used computerized image analysis and machine learning approaches to characterize architectural immune patterns in lung H&E digitized tissue images from patients who died of COVID-19; specifically, we analyzed the lymphocyte spatial distribution and its relation with surrounding nucleated cells. Additionally, we sought to tease out differences in this spatial arrangement between COVID-19 and H1N1, a comparable viral disease

**Design:** H&E lung whole slide images from 9 COVID-19 and 2 H1N1 patients were computationally interrogated. 606 image patches (~55 per patient) of 1024X882 pixels were extracted from the 11 autopsied patient studies. After color normalization, a watershed-based segmentation approach in conjunction with a machine learning classifier was employed to identify two types of cell families: lymphocytes and non-lymphocytes (i.e. other nucleated cells such as pneumocytes, fibroblasts, macrophages, neutrophils) (Fig 1). Based on the proximity of the individual cells, cell clusters for each cell type were constructed. For each of the resulting clusters, a series of quantitative measurements relating to architecture and density of cell clusters were calculated. Finally, different statistical approaches were employed to study differences in immune patterns

**Results:** In comparison to H1N1, COVID-19 immune response showed fewer lymphocytes per patch and multiple but smaller sized lymphocyte clusters (Wilcoxon  $p < 0.05$ ). Additionally, COVID-19 consistently showed regions encompassed by lymphocyte clusters typically overlapping with non-lymphocyte clusters. H1N1 autopsied tissue images presented few but very large clusters of non-lymphocytes. Fig 2 shows representative patches of COVID-19 (yellow border) and H1N1 (red border); lymphocyte clusters are represented in blue and non-lymphocyte in green and violin plots comparing features

Figure 1 – 789

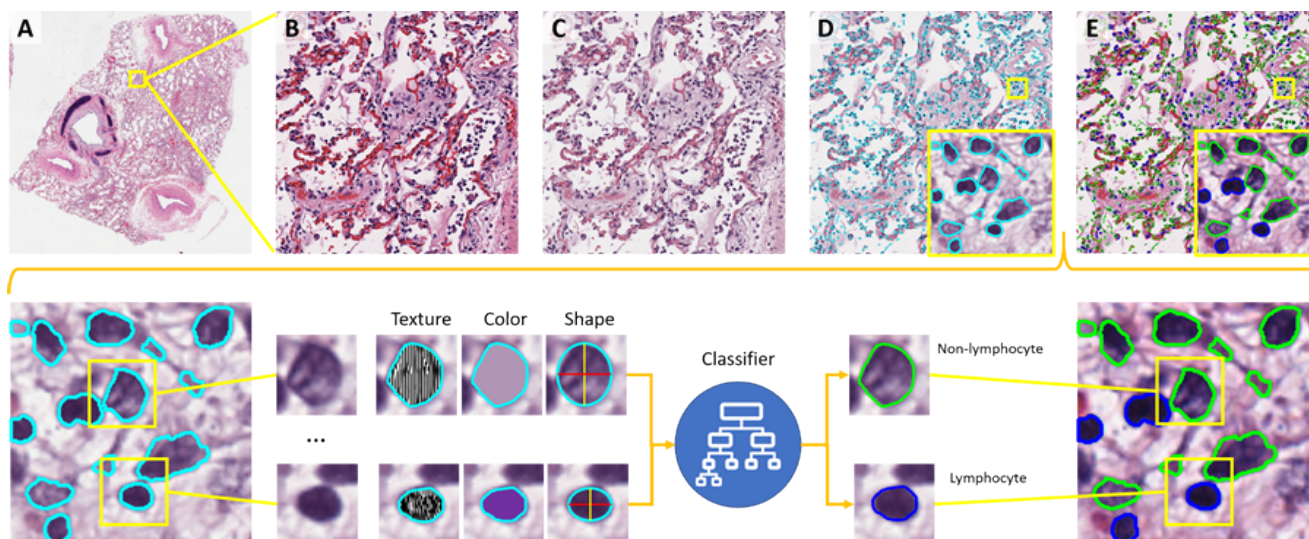
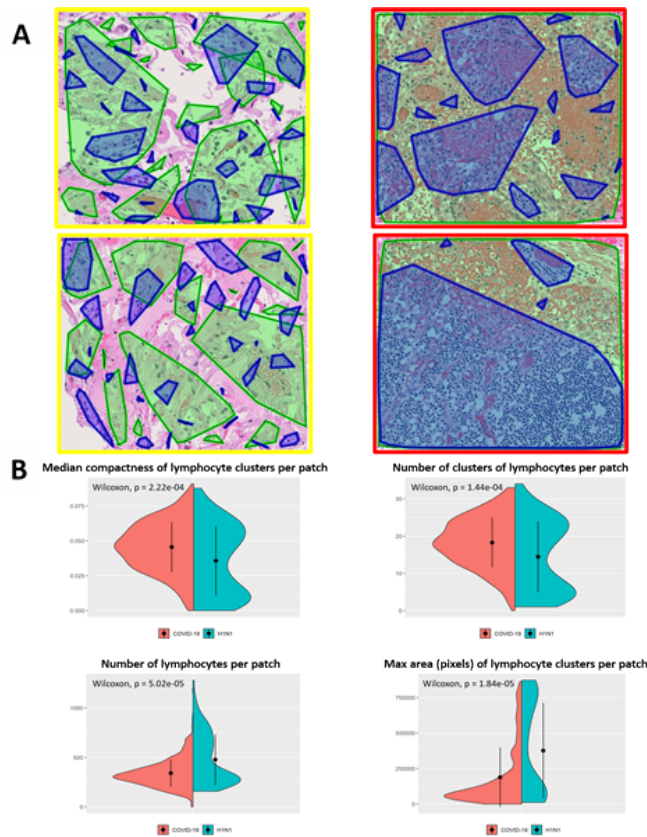


Figure 2 – 789



**Conclusions:** COVID-19 and H1N1 exhibit different immune spatial architecture patterns. The former showed a lymphocyte response rather modest, possibly as an expression of the constantly reported lymphocytopenia. The latter exhibited an emphatic response of non-lymphocytes, a possible reflection of increased non-lymphocytic response.

**790 AI Identification of Placental Regions from Whole Slide Images**

Brian Vadasz<sup>1</sup>, Huma Khan<sup>2</sup>, Payal Patel<sup>2</sup>, Lee Cooper<sup>3</sup>, Jeffery Goldstein<sup>4</sup>

<sup>1</sup>McGaw Medical Center of Northwestern University, Chicago, IL, <sup>2</sup>Northwestern University, Evanston, IL, <sup>3</sup>Northwestern University, Chicago, IL, <sup>4</sup>Feinberg School of Medicine/Northwestern University, Chicago, IL

**Disclosures:** Brian Vadasz: None; Huma Khan: None; Payal Patel: None; Jeffery Goldstein: None

**Background:** The placenta is a key driver of diseases of pregnancy and abnormalities in the placenta reflect life-long risk of disease in the mother and infant. Machine learning on scanned whole slide images (WSI) has the potential to decrease interobserver variability and improve reliability of diagnosis. Correct identification of placental regions is foundational for diagnosis. Many findings have a differing significance based on their location. For example, thick walled arterioles in the decidua are evidence of pathologic failure to remodel maternal vessels, while they are normal in fetal stem villi. We sought to determine whether region identification is a tractable problem for machine learning.

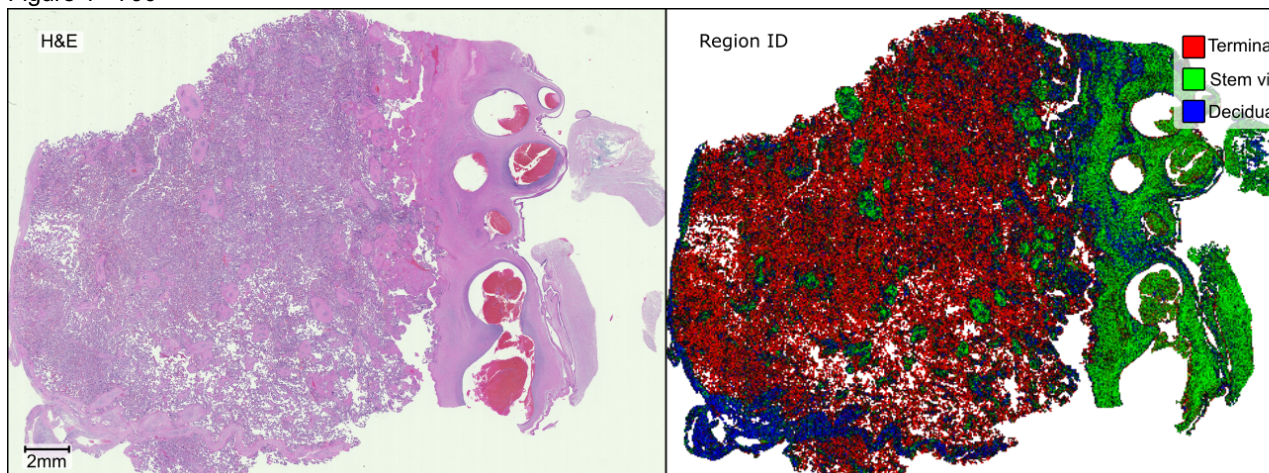
**Design:** 190 whole slide images (WSI) of placenta of varying gestational age but otherwise without significant histologic abnormality were studied. Rectangular annotations of terminal villi, stem villi, and decidua were made. Regions were extracted and randomly split 50:25:25 into training:validation:test sets. Regions were randomly cropped to 128x128 pixel high power fields (HPF). HPF were input to a deep learning network based on MobileNetV2 with pretrained weights. Categorical accuracy was measured. For whole-slide region identification,

128x128 hpf were generated across the whole slide and identified using the trained network. The resulting logits for terminal villi, stem villi, and decidua were used as the red, green, and blue intensity values (respectively). Non-tissue areas were masked using Otsu’s method. IRB approval was obtained, STU00211333.

**Results:** After 25 epochs, we demonstrated a categorical accuracy of 0.83 in the test set (Table). Accuracy was 0.92 for terminal villi, 0.68 for stem villi and 0.92 for decidua. To examine the performance of the network, we generated region identifications for all tissue HPF in a single whole slide image (Figure, left panel: H&E, right panel: AI classification of region type). Disc parenchyma is primarily terminal villi (red) with intermixed stem villi (green). The chorionic plate (right side of tissue) is identified as stem villous-like, reflecting its fibrous stroma and large blood vessels. Basal plate is correctly identified as decidua (blue, left side of tissue), however subchorionic fibrin is also (incorrectly) identified as decidua.

			AI call (%)	
		Decidua	Stem villi	Terminal villi
	Decidua	91	4	5
Actual (%)	Stem villi	13	68	19
	Terminal villi	4	3	92

Figure 1 - 790



**Conclusions:** These results demonstrate that placental microanatomy is readily machine-recognizable. This step is foundational for identification of diseases and processes where diagnosis is dependent on the region, e.g. decidual arteriopathy vs. normal fetal arterioles.

**791 An Adaptive, Collaborative, Efficient, and Precise Image Annotation Method for Difficult Morphologic Features in Deep Learning**

Keluo Yao<sup>1</sup>, Bradley Stohr<sup>2</sup>, G. Zoltan Laszik<sup>2</sup>

<sup>1</sup>City of Hope Cancer Center, Duarte, CA, <sup>2</sup>University of California, San Francisco, San Francisco, CA

**Disclosures:** Keluo Yao: None; Bradley Stohr: None; G. Zoltan Laszik: None

**Background:** The current annotation methods for histopathologic images for deep learning rely on anatomic pathology domain experts to mark regions of interest (ROI) with geometric or arbitrary boundaries. Such methods can be labor intensive, imprecise, and difficult to scale to multiple annotators to construct training data for machine learning algorithms. This study aims to develop an alternative method that allows adaptive, collaborative, efficient, and precise annotation of histologic features with difficult to define boundaries.

**Design:** Instead of creating ROI to establish boundaries between histologic features, we opted to design the method based on the annotation of standardized image tiles that contain the histologic features of interest. The annotators view the individual image tiles in the context of the entire image and are asked to bin the image tiles into a pre-defined category. To test this method, we developed a tool based on web application technologies (JavaScript and virtualization container) that serve image tiles to annotators. The annotations are recorded by a database (PostgreSQL). We deployed the initial version of the tool to support the development of an algorithm for prostate cancer (Figure 1). The algorithm is designed based on a pre-trained VGG16 convolutional neural network and receives 256 by 256 pixel image tiles as input. The image tiles are decomposed from whole slide images (in MIRAX format) at the lowest magnification level (40x).

**Results:** Using training (152592 tiles), testing (4769 tiles), and validation images (364 tiles) annotated by the tool, we transfer trained and fined tuned the algorithm to achieve up to 82% accuracy in predicting an image tile as 1) benign or 2) atypical or neoplastic.

Figure 1 - 791

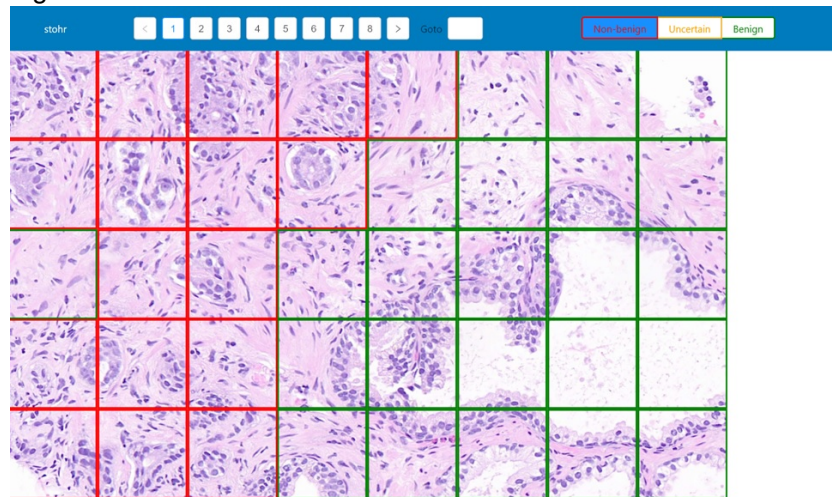


**Figure 1:** We developed a tool to annotate histopathologic images based on standardized image tiles to allow better annotation of difficult morphologic features. The annotators simply select a classification category and click on the appropriate image tiles that contain the histologic feature of interest.

**Conclusions:** We successfully designed a novel method for annotating histologic features and deployed it using web application technologies. The initial version shows it can be successfully used to annotate prostate cancer with difficult to annotate atypical features and develop a large quantity of training, testing, and validation data successfully. The use of flexible web application technologies will allow adaptive and collaborative functions to be developed in the next phase.

**792 Curbside Consults for Soft Tissue Pathology Using Whole Slide Images**

Mustafa Yousif<sup>1</sup>, Caylin Hickey<sup>2</sup>, Mauricio Zapata<sup>3</sup>, Therese Bocklage<sup>2</sup>, Bonnie Balzer<sup>4</sup>, Marilyn Bui<sup>5</sup>, Jerad Gardner<sup>6</sup>, Cody Bumgardner<sup>2</sup>, Liron Pantanowitz<sup>7</sup>, Shadi Qasem<sup>8</sup>

<sup>1</sup>Michigan Medicine, University of Michigan, Ann Arbor, MI, <sup>2</sup>University of Kentucky College of Medicine, Lexington, KY, <sup>3</sup>Northside Hospital, Atlanta, GA, <sup>4</sup>Cedars-Sinai Medical Center, Los Angeles, CA, <sup>5</sup>H. Lee Moffitt Cancer Center & Research Institute, Tampa, FL, <sup>6</sup>Geisinger Medical Center, Danville, PA, <sup>7</sup>University of Michigan, Ann Arbor, MI, <sup>8</sup>University of Kentucky School of Medicine, Lexington, KY

**Disclosures:** Mustafa Yousif: None; Caylin Hickey: None; Mauricio Zapata: None; Therese Bocklage: None; Bonnie Balzer: None; Marilyn Bui: None; Jerad Gardner: None; Cody Bumgardner: None; Liron Pantanowitz: None; Shadi Qasem: None

**Background:** “Curbside consults” are informal consults where pathologists show their peers representative slide(s) from challenging cases with limited information or workup, with the intention to get a definitive diagnosis, ideas for possible diagnosis or suggested further workup. Digitally, pathologists have used photos taken by cell phones or



microscope-mounted cameras for this purpose. The aim of this study was to evaluate the use of whole slide images (WSI) in a similar manner for challenging soft tissue cases.

**Design:** Five soft tissue pathologists from 5 separate medical centers, independently reviewed 100 WSI of hematoxylin and eosin-stained slides representing 100 different soft tissue cases. Only 1 slide per case was provided with limited clinical information (patient age, gender and anatomic location). Slides were scanned using an Aperio scanner at 20X magnification. Images were converted from .SVS to DICOM format and uploaded to a locally-hosted, externally-accessible compute node for review using a web-based WSI viewer (Orthanc v1.3.2 WSI Plugin v0.5) web-based WSI viewer system. Pathologists were asked to choose one of four diagnostic categories: (benign, intermediate/borderline, malignant, uncertain), and to provide up to 3 differential diagnoses. A REDCap survey was used to record answers. Answers were compared to the original “reference” diagnosis.

**Results:** Compared with the reference diagnosis, the group’s overall concordance rate, using the 4 diagnostic categories, was 70.4%. Minor discordance was seen in 11.6% of cases and major discordance in 5%. There was uncertainty in 13% of cases. When looked at separately, malignant cases had the highest concordance rate (81.7%), benign cases had the highest major discordance rate (7.7%), and intermediate cases had the highest minor discordance (28%) and uncertainty rates (22.4%). Overall, the correct differential was rendered in 63% of the cases. Pathologists reported excellent or satisfactory quality of scanning in 96.4% of cases. [Table1]

Pathologists (P)	Overall Concordance Rate (%)	Major Discordance (%)	Minor Discordance (%)	Uncertain Diagnosis (%)	Correct DX (%)
P1	70	5	10	15	66
P2	71	3	8	18	70
P3	70	4	9	17	63
P4	76	9	15	0	37
P5	65	4	16	15	79
<b>Overall</b>	70.4	5	11.6	13	63

**Table 1:** Summary of study findings. “Concordance” indicates agreement with the reference diagnosis with regards to the diagnostic categories (benign, intermediate/borderline and malignant). Correct diagnosis is recorded when one of the differentials provided by the pathologist matches the reference diagnosis (e.g. myxoid liposarcoma).

**Conclusions:** Despite limited clinical information, having only one slide to review and no ancillary testing results, expert pathologists had a relatively low major discordance rate, and they were able to suggest the correct diagnosis in two thirds of cases. Intermediate/borderline is the hardest category to classify. Despite the challenging nature of soft tissue pathology, WSI is a suitable for “curbside consults”. It is necessary to review all the slides for a case and have access to immunohistochemical and molecular studies in order to make the correct soft tissue diagnosis.

**793 Correlation Between Quantitative Image Analysis and Manual Scoring of ER, PgR, and HER2/neu in Invasive Breast Carcinoma**

Mustafa Yousif<sup>1</sup>, Yiyuan Huang<sup>2</sup>, Andrew Sciallis<sup>2</sup>, Celina Kleer<sup>2</sup>, Judy Pang<sup>2</sup>, Brian Smola<sup>3</sup>, Kalyani Naik<sup>3</sup>, David McClintock<sup>2</sup>, Lili Zhao<sup>2</sup>, Liron Pantanowitz<sup>2</sup>

<sup>1</sup>Michigan Medicine, University of Michigan, Ann Arbor, MI, <sup>2</sup>University of Michigan, Ann Arbor, MI, <sup>3</sup>Michigan Medicine, Ann Arbor, MI

**Disclosures:** Mustafa Yousif: None; Yiyuan Huang: None; Andrew Sciallis: None; Celina Kleer: None; Judy Pang: None; Brian Smola: None; Kalyani Naik: None; David McClintock: None; Lili Zhao: None; Liron Pantanowitz: None

**Background:** Evaluation of biomarker expression for estrogen receptor (ER), progesterone receptor (PgR), and human epidermal growth factor receptor 2 (HER2/neu) are essential prognostic and predictive parameters for breast cancer and critical for guiding hormonal and neoadjuvant therapy. Quantitative image analysis (QIA) of these biomarkers has been advocated to generate more reproducible and accurate results than manual assessments. To

the best of our knowledge, this study is one of the largest aimed to compare QIA with pathologists' scoring for ER, PgR, and HER2/neu.

**Design:** A retrospective analysis was undertaken of 1443 invasive breast carcinomas, including all histopathology subtypes, for which ER, PgR, and HER2/neu were analyzed by manual scoring and QIA. All immunostains were performed using an automated immunostainer (Ventana, Roche). Immunohistochemical glass slides were scanned (Ventana iScan Coreo, Roche) and regions of interest from whole slide images subsequently analyzed by trained cytotechnologists using image analysis software (Ventana Virtuoso, Roche). QIA scores were compared with pathologist's manual scores, and in a subset of HER2/neu cases (n=373, 26%) scores were correlated with available FISH results.

**Results:** Concordance between QIA and manual scores for ER was 97%, PgR was 96%, and HER2/neu was 93%. The majority of discordant cases for ER (n=33) had low positive scores (1-10%), except in 2 cases with >80% positive tumor nuclei due to intermingled ductal carcinoma in situ (DCIS). The majority of discordant cases for PgR (n=43) were due to non-representative region selection (e.g. DCIS) or tumor heterogeneity. The majority of discordant cases for HER2/neu (n=90) were of only one-step difference (negative to equivocal, equivocal to positive, or vice versa), except in two false positive QIA cases where DCIS was incorporated. Among HER2/neu cases where FISH results were available, only 4 (1.0%) showed discordant QIA and FISH results.

**Conclusions:** Quantitative image analysis is a helpful diagnostic support tool for our pathologists that significantly improves standardization of ER, PgR, and HER2/neu scoring. QIA for all three breast carcinoma biomarkers demonstrated excellent concordance with pathologists' scores and accurately discriminated between HER2/neu FISH positive and negative cases. To avoid pitfalls, such as including areas of DCIS for image analysis, pathologist oversight of representative region selection in each case is recommended.

**794 A Rapid Technique to Address Recall Bias Without a 2-Week Antegrade Washout Period in the Validation of Whole Slide Imaging for Histopathological Primary Diagnosis**

Christopher Zarbock<sup>1</sup>, Angella Coffee<sup>2</sup>, Paari Murugan<sup>1</sup>, Mark Luquette<sup>1</sup>, Molly Klein<sup>1</sup>, Lihong Bu<sup>1</sup>, Faqian Li<sup>1</sup>, Mahmoud Khalifa<sup>1</sup>, Oyedele Adeyi<sup>1</sup>

<sup>1</sup>University of Minnesota, Minneapolis, MN, <sup>2</sup>University of Minnesota Medical Center, Minneapolis, MN

**Disclosures:** Christopher Zarbock: None; Angella Coffee: None; Paari Murugan: None; Mark Luquette: None; Molly Klein: None; Lihong Bu: None; Faqian Li: None; Mahmoud Khalifa: None; Oyedele Adeyi: None

**Background:** Digital pathology has gained much traction in recent years given the improvement in whole slide imaging (WSI) technology and recent FDA approval for primary diagnosis. A critical component in the adoption of digital pathology for clinical use is the demonstration of non-inferiority to conventional glass slide diagnosis. Eliminating recall bias has always been a challenge in such a validation process. To minimize this, the current CAP guidelines recommend a 2-week period between switching from one to the other diagnostic modality. A 2-week 'washout period' was selected as it best combined practicality with diagnostic concordance when comparing washout periods of 1 week, 2-3 weeks, and ≥ 6 months. While many believe 2 weeks is still too short an interval, even this adds considerable validation time. The impact of this additional time was particularly significant during the early days of COVID-19 given the need for rapid validation following the CMS waiver allowing remote pathology sign-out. In an effort to streamline the validation process, we devised an approach that substituted a prospective for a retrospective washout period while still minimizing recall bias.

**Design:** Slide digitization was performed at 20x magnification with the Leica Aperio AT2 for 20 H&E slides comprising 20 cases and 38 special stains slides comprising 20 additional cases (Table 1). Each set of cases was representative of the complexity and spectrum of those encountered in our practice. All cases selected for review had been signed-out in the preceding 3 weeks to 2.5 years with most completed within the preceding 6 months. Each case was assigned a new identifier unlinked to the original accession which blinded pathologists to the initial case. Pathologists were provided the same clinical data as at initial review and reporting was done within the same LIS. For greater than 90% of these cases, pathologists reevaluated digital slides for the same cases they had previously completed. Concordance was defined as the same diagnosis, staging (e.g. fibrosis with trichrome), and/or positive/negative as indicated. We targeted a concordance rate of ≥ 95% per the CAP WSI validation guidelines.

**Results:** There was 100% concordance (20/20) for H&E and 97.4% (37/38) concordance for special stains (GMS WSI outperformed the glass slides in one case later confirmed to have been a false negative on the glass slide) (Table 1).

Table 1: Tissue type, corresponding stains, and concordance for each case involved in the validation process.

Tissue type	Stains	Concordant
Bladder biopsy	H&E	Yes
Liver biopsy, CT-guided	H&E	Yes
Soft tissue mass	H&E	Yes
Kidney biopsy	H&E	Yes
Prostate	H&E	Yes
Lung mass	H&E	Yes
CT-guided lung biopsy	H&E	Yes
Lingula and lung biopsies	H&E	Yes
Lung wedge	H&E	Yes
Lung biopsy	H&E	Yes
Breast biopsy	H&E	Yes
Breast biopsy	H&E	Yes
Stereotactic breast biopsy	H&E	Yes
Breast biopsy	H&E	Yes
Uterus	H&E	Yes
Rectum	H&E	Yes
Liver resection, gallbladder	H&E	Yes
Liver resection	H&E	Yes
Liver needle biopsy	H&E	Yes
Liver needle biopsy	H&E	Yes
Lung wedge	GMS	Yes
Liver resection	PAS, GMS	Yes
Liver needle biopsy	Iron, retic, trichrome, PAS	Yes
Liver needle biopsy	PAS, trichrome, retic	Yes
Kidney biopsy	PAS, trichrome, Jones	Yes
Kidney biopsy	PAS, trichrome, Jones	Yes
Kidney biopsy	PAS, trichrome, Jones	Yes
Soft tissue	GMS	No (WSI positive for fungus not seen initially on glass slide)
Skin	GMS	Yes
Soft tissue	GMS	Yes
Prostate biopsy	Mucicarmine	Yes
Liver needle biopsy	Retic, trichrome	Yes
Soft tissue biopsy	GMS	Yes
Liver needle biopsy	Retic, trichrome	Yes
Liver needle biopsy	Retic, trichrome	Yes
GI biopsies	GMS	Yes
Liver needle biopsy	PAS-D, retic, trichrome	
Tongue biopsy	PAS, GMS	Yes
Temporal artery biopsy	EVG	Yes
Temporal artery biopsy	EVG	Yes

**Conclusions:** The described method facilitates rapid validation of H&E and special stains for primary diagnosis via WSI by utilizing expired time to minimize recall bias rather than any future washout period. This approach also addresses the uncertainty of the best length for washout, since it allows extension beyond 2 weeks (up to 2.5 years in this study). Our approach therefore enables validation to be accomplished in a matter of days with potentially improved elimination of recall bias.